Renewable Energy 180 (2021) 893–913

Contents lists available at ScienceDirect

Renewable Energy

journal homepage: www.elsevier.com/locate/renene

Sustainability insights on emerging solar district heating technologies to boost the nearly zero energy building concept

Mohamed Hany Abokersh [a, b], Sachin Gangwar [c], Marleen Spiekman [d], Manel Vallès [a], Laureano Jiménez [c], Dieter Boer [a, *]

[a] Departament d'Enginyeria Mecànica, Universitat Rovira i Virgili, Av. Països Catalans 26, 43007, Tarragona, Spain
[b] Departament of Sustainable Manufacturing, Irish Manufacturing Research, Collegeland, Rathcoole, Co, Dublin, D24 WC04, Ireland
[c] Departament d'Enginyeria Química, Universitat Rovira i Virgili, Av. Països Catalans 26, 43007, Tarragona, Spain
[d] Department of Building Physics and Systems, TNO, Leeghwaterstraat 44, Delft, the Netherlands

ARTICLE INFO

Article history:
Received 26 April 2021
Received in revised form
3 August 2021
Accepted 24 August 2021
Available online 1 September 2021

Keywords:
Solar assisted district heating system
Nearly zero energy building
Life cycle assessment
Multi-objective optimization
Multi-criteria decision making
Sustainability targets

ABSTRACT

Arising the Nearly Zero Energy Buildings (NZEB) concept in Europe, the solar district heating systems (SDHS) present a potential solution to meet the buildings sector's European energy performance directive. Nevertheless, current practices face several technological and economical barriers to ensure service quality. In this context, our work presents a sustainability analysis (technical, economic, environmental, and social) for SDHS integration in the residential sector to meet the NZEB and positive energy building goals. This paper proposes an application of a machine learning model incorporating multi-objective optimization and multi-criteria decision making to facilitate a sustainability index for the decision-making stakeholders and policymakers. The proposed analysis application is illustrated through retrofitted residential communities with building energy rating (D) at different sizes (10, 25, 50, 100, and 500 houses) located in Emmen (Netherlands) and compared to a standard decentralized heat pump. The optimization results show the ability of SDHS to provide a solar fraction up to 95% in the community of 500 houses. Furthermore, achieving a NZEB status is only approved economically from a community size of 100 houses with a life cycle cost of 41 €/m^2 and a payback period of 25 years. These results align with a substantial environmental and social improvement of 78.2% and 29.7%, respectively, compared to the decentralized heat pump. Overall, this study provides policy decision making with an evaluation for positive energy communities and suggests the SDHS integration to meet the global sustainability goals.

1. Introduction

The world population is expected to consume 50% more energy by 2035 (compared to 1990) due to rapid growth in population, infrastructure, technology, and energy-intensive systems. This aspect has a direct impact on building energy consumption [1]. In the European Union (EU), the building sector alone accounts for approximately 40% of total energy consumption and 36% of the total CO_2 emissions [2]. Consequently, a more sustainable and climate oriented efficient building stock is needed to achieve climate-neutral Europe's goals by 2050. Corporations in the infrastructure industry face an urgent need to change their traditional practices in terms of energy access and its use to reduce building stocks' energy needs. International bodies set guidelines to follow the nearly zero energy building (NZEB) route. The NZEB concept is vastly interpreted as the utilization of renewable energy to satisfy building energy need. Sustainable energy authority of Ireland defines NZEB as '*a building that has a very high energy performance, and the nearly zero or very low amount of energy required should be covered to a very significant extent by energy from renewable sources, including energy from renewable sources produced on-site or nearby*' [3]. However, communities worldwide have not yet reached a consensus on the definition [4]. National Renewable Energy Laboratory of the United States has classified NZEB as a range of buildings, e.g., from a building that offsets all of its energy needs from renewable energy resources available on-site' to a building that achieves an NZEB status through a combination of on-site renewables and off-site purchases of renewable energy credits

* Corresponding author.
E-mail addresses: mohamed.abokersh@urv.cat (M.H. Abokersh), sachin.gangwar@urv.cat (S. Gangwar), marleen.spiekman@tno.nl (M. Spiekman), manel.valles@urv.cat (M. Vallès), laureano.jimenez@urv.cat (L. Jiménez), dieter.boer@urv.cat (D. Boer).

https://doi.org/10.1016/j.renene.2021.08.091

Nomenclature

$Cap_{heating}$	Energy supplied by heat pump (MWh)
C_{el}	Buying the grid electricity price (€/MWh)
C_{ng}	Natural gas price (€/MWh)
d	Discount rate (%)
DAM_d	Endpoint score for environmental damage category (−)
EC_{RE}	Electricity generated by PV array (MWh)
EG_S	Electricity purchased from the grid (MWh)
EO	Employment opportunity (−)
G_{value}	Windows solar energy transmittance (−)
IC	Capital cost of the SDHS (M€)
i_{ng}	Natural gas inflation rate (%)
i_e	Electricity inflation rate (%)
i	Inflation rate (%)
LCC	Life cycle cost (€)
NPC	Net present cost (€/m^2)
OC	Operational cost of SDHS (M€)
PBT	Payback time (years)
Q_{AUX}	Total thermal energy demand supplied by auxiliary units (MWh)
$\dot{Q}_{AUX_1}$	Thermal power supplied by auxiliary heater 1 (MW)
$\dot{Q}_{AUX_2}$	Thermal power supplied by auxiliary heater 2 (MW)
$Q_{DHW\ load}$	Total thermal energy demand for hot water (MWh)
$Q_{electric\ load}$	Total electricity demand (MWh)
$Q_{SH\ load}$	Total thermal energy demand for space heating (MWh)
Q_{total}	Total energy consumption (MWh)
R_{fuel}	The ratio of total energy supplied by fossil fuels (−)
RC	The replacement cost of SDHS (M€)
RC_{roof}	Thermal resistance of the roof (m^2·K/W)
RC_{floor}	Thermal resistance of the floor(m^2·K/W)
RC_{facade}	Thermal resistance of the façade (m^2·K/W)
RCP	Normalized indicator metric for environmental damage (Pt./m^2)
REF_{elec}	Renewable energy fraction for electrical energy (−)
REF_{th}	Renewable energy fraction for thermal energy (−)
R_{HP}	The ratio of total energy supplied by the heat pump (−)
RC_{roof}	Thermal resistance of the roof (m^2·K/W)
RC_{floor}	Thermal resistance of the floor (m^2·K/W)
RC_{facade}	Thermal resistance of the façade (m^2·K/W)
U_{glass}	U-value of windows W/(m^2·K)
S_{el}	Selling to the grid electricity price (€/MWh)
σ	Percentage variance contribution (%)

Abbreviations

ANN	Artificial neural network
DH	District Heating
DHWT	Domestic hot water tank
EPBP	Energy performance building parameter
EPI	Energy performance indicator
4GDH	4th generation district heating
GHG	Greenhouse gas emissions
GSA	Global sensitivity analysis
HP	Heat pump
KNMI	Royal Netherlands Meteorological Institute
LCB	Low carbon buildings
LCIA	Life Cycle Inventory Analysis
MCDM	Multi-criteria decision making
MOO	Multi-objective optimization
MOGA	Multi-objective genetic algorithm
NZEB	Nearly-zero energy building
PEB	Positive energy building
PV	Photovoltaic
SDHS	Solar assisted district heating system
SH	Space heating
SST	Seasonal storage tank
TOPSIS	Technique for Order of Preference by Similarity to Ideal Solution

[5]. The Energy Performance of Building Directive (EPBD) from the EU, requires all new buildings to be NZEB from 2021 and aims to achieve a highly decarbonized building stock by 2050 for existing and new buildings (Directives 2010/31/EU and 2018/844/UE) [6]. Driving forces for the rise of NZEBs have been explained in detail elsewhere [7], showing the social, economic and environmental benefits. To achieve this transition, centralized and decentralized renewable energy usage can push nearly-zero energy buildings. Currently, Europe has 70% of the building stock needed by 2050 and improving the existing building stock's energy efficiency is an effective way to reduce energy demand [8], so this paper focuses on installable renewable energy solutions to satisfy the energy demand on building stock [9].

The transition of existing building blocks towards NZEB can be achieved by improving the building's energy efficiency, equipping the building block with renewable energy generation sources and connecting the building block with the district heating (DH) network. 4th generation district heating (4GDH) network is a promising concept to reduce high energy losses and installation and maintenance cost of previous generations district heating systems [10,11]. The high performance of 4GDH is attributed to its low-operation temperature (50–60 °C). However, more research is required for the broad implementation of 4GDH [12,13]. The use of renewable energy technology and DH networks can reduce the building block's carbon footprint and, thus, building blocks with low carbon emission are called Low Carbon Buildings (LCB), building blocks with nearly-zero carbon emission called Nearly Zero Energy Building (NZEB). A plethora of research is available on the NZEB with different energy sources and different perspectives. While some of the researchers have used photovoltaics, solar thermal systems, geothermal systems [14,15], others have tried to measure the prospects of conventional smart energy systems and net metering [13]. While the research has been catching up to the target of carbon neutrality and the NZEB concept [16], some researchers have also developed positive energy buildings (PEBs). PEB essentially means that the building or the building stock can satisfy its energy demand and be able to produce more energy to supply to the centralized district heating (DH) network (thermal energy) or the grid (electrical energy). Research in PEB is still in its nascent stage, and till now very few researchers have tried to make the transition from low carbon buildings to nearly zero energy buildings to positive energy buildings [17]. The concept of integrating smart energy systems to connect the building stock with grid and district heating network has also been studied [18] and the technical feasibility of the building stock [19]. The smart energy system is a broader concept which suggests the load reduction on the electrical grid by connecting the demand to the respective energy networks (i.e., electricity demand to the electricity grid,

heating demand to district heating networks, etc.). Smart energy system also incorporates the concept of net metering, thereby addressing the component of direct financial benefit to the user for the implementation of such a system. The futuristic vision of high energy performance building stock can be achieved with smart energy system integration, especially in cold regions, by connecting to 4GDH [20]. To implement EPBD regulations towards the NZEB transition, the Netherlands set the guidelines for achieving energy efficiency and the building's rating [6]. These indicators collectively form "EPC" (energy performance coefficient), which standardize the process of building energy efficiency rating [21].

Netherlands has a high potential for retrofit residential building stock and connects to renewable energy sources to reduce greenhouse gas emissions (GHG) [22]. Numerous efforts are being made to satisfy building energy consumption by renewable energy system installation (e.g., rooftop PV [23], geothermal heat pumps [24], solar-assisted heat pumps [25], passive heating and cooling [26]). Researchers have analyzed from the life cycle perspective [27] building integrated solutions with photovoltaics (PV) [28], increased renewable energy input with multiple systems [29], comprehensive solar energy solutions with PV and flat plate collectors [30] to satisfy the energy demand of the building and to assess the greenhouse gas emission. Extensive research has been done on case studies related to the application of photovoltaics [1], solar thermal applications [31] and technological design option for PV [32] in NZEBs and low carbon energy buildings. Given the environmental benefits associated with renewable energy utilization in buildings, a global rise has been observed in the area of NZEB and the low-carbon buildings (LCBs) application and research [4].

The availability of various green energy solutions has led to the adoption of different approaches by the researchers. In attempts to reach NZEB status, Dawood et al. [33] suggested a framework that includes the integration of energy simulation tools, national calculation methods and codes for low carbon buildings (LCB) and multi-criteria decision making (MCDM) to support the building design process. However, this framework was specifically addressing the architects for retrofitting. To emphasize the impact of various key areas, researchers have also used MCDM: for energy systems design optimization to encounter load uncertainty [34], for building design optimization methods [35], for assessment and ranking of renewable energy technology [36] to point out the key decision-makers. Hang et al. [37] has summed up the findings of major agencies and researchers to move from low carbon buildings to NZEB: (i) assessing the energy and GHG emissions; (ii) optimizing the on-site and off-site distribution of renewable energy; (iii) answering low carbon buildings (LCB) potentials through high-performance energy end-use devices and occupants' green behavior.

Achieving NZEB or PEB status for a building requires optimization of numerous variables (e.g. selection of an optimal renewable energy technology [38], optimizing building energy design [39], optimizing the use of energy-efficient material) [40]. Classical and metaheuristic optimization methods are not able to effectively optimize a large number of variables simultaneously as require large computational resources. Optimizing a multivariate objective function is difficult for non-confluent variables with mathematical programming, and some researchers use machine learning [41]. With the use of machine learning, Rehman et al. [42] analyzed and optimized a building integrated photovoltaic panel, battery and use of electric vehicles in central European climatic condition, Han et al. [43] optimized the fault diagnosis of a building energy system, and Salah et al. [44] predicted the building energy performance to support deep energy retrofit. The use of machine learning by various researchers has been reviewed by Fathi et al. [45] in urban building energy performance forecasting, by Mishra [46] for structural health monitoring of heritage buildings, by Sun et al. [47] for building structural design and performance assessment, by Ayoub [48] to predict daylighting inside buildings and by Hong et al. [49] in the area of building life cycle. The use of machine learning in energy systems design, sizing and techno-economic analysis and environmental analysis to achieve NZEB targets is yet to be explored. We have used a machine learning approach based on an artificial neural network (ANN) to optimize a multi-objective function that incorporating economic, environmental, and social variables. The robustness of these optimization approaches can be investigated with a global sensitivity analysis (GSA) against the uncertain parameters. GSA is an extensive tool to identify the major parameters causing uncertainty into an optimization model. Mavromtidis et al. [50] used GSA to determine the major causes of variation in economic and energy performance optimization of a distributed energy system. The use of GSA to provide the cushion against parameter uncertainty in energy system design is extensive [51]. Zhang et al. have used GSA or key parameters identification of net-zero energy buildings for grid interaction optimization [52]. Hence, machine learning in conjugation with GSA is gaining popularity for energy systems optimization under uncertainty for NZEB.

The available literature on NZEB unanimously recommends the integration of renewable energy into building footprints. Therefore, we aim to achieve the PEB targets by retrofitting a building stock situated in North-East Netherlands (Emmen). We are trying to achieve PEB status following the 4GDH principles to satisfy the heating and adding a rooftop PV system to meet the building stock's electricity demand. In addition, we connected the model to the electricity grid and centralized DH network.

Hence, this work's novelty lies in demonstrating the sustainability aspects for integrating 4GDH at various residential community sizes located in the Netherlands to achieve NZEB targets. Additionally, this paper develops a MCDM framework based on optimal scenarios to support the selection of the most sustainable system design at various residential community size. This work suggests a roadmap for a transition from LCBs to PEBs with the integration of seasonal storage, heat pumps, PV, and smart energy systems. The structure of this article is as follows: section 2 shows a complete description of the 4GDH system and neighbourhood demand. Section 3 describes the sustainable criteria to evaluate the DH performance. The ANN model's mathematical description and its coupling with a multi-objective optimization framework are presented and discussed in section 4. The post-analysis of the optimal solutions, including the MCDM and GSA, is shown in Section 5. Section 6 offers the required results and discussion. Finally, the work summary and conclusion are shown in section 7.

2. System description

2.1. Roof-mounted hybrid solar assisted district heating

A typology of solar assisted district heating system (SDHS) combined with heat pump (HP) is designed for a residential neighbourhood in the Netherlands to supply yearly demand of space heating (SH), domestic hot water (DHW) and electricity, as shown in Fig. 1. This system primarily incorporates roof-mounted solar thermal collectors (ST) and photovoltaic panels (PV), a seasonal thermal storage tank (SST), a domestic hot water tank (DHWT), central water to water HP unit, and auxiliary heaters fuelled by natural gas. HP serves as a heat input source for both SST and DHWT. For this arrangement, heat collected via the ST is used to meet SH/DHW demand, where the heat is transferred across the distribution network through heat exchangers using 'Y' valves. Contingent to operational mode, the heat produced by HP is either

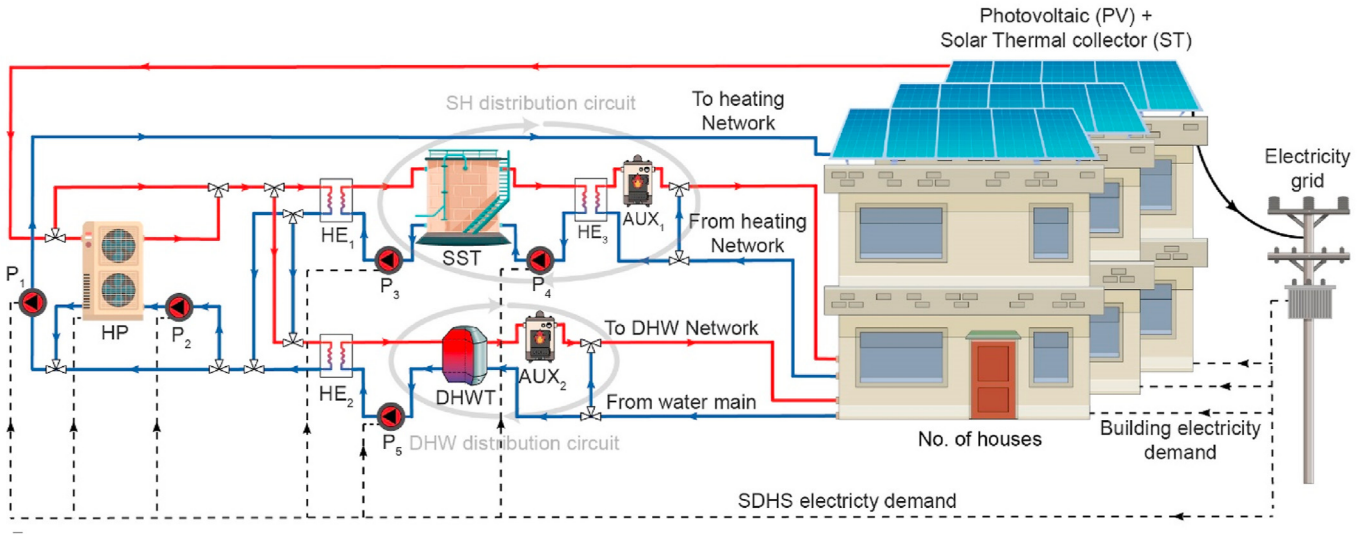

Fig. 1. Schematic of roof-mounted hybrid solar assisted district heating network.

used for SH or DHW with potential application for SST heat charging. For the winter season, the SST is used to satisfy SH demand, whereas short-term DHWT meets the daily DHW. The heat is supplied at low-temperature (50 °C) for space-heating, while the heat to DHW is supplied at higher-temperature (60 °C). Lastly, when solar collectors, HP and SST are not able to satisfy the heat load, the disparity is overcome via auxiliary heaters. On the other hand, the electricity demand comprising both the neighbour and SDHS electric equipment is covered by a combination of the on-grid roof-mounted PV panels and the electricity grid.

An efficient control strategy is adopted to meet the residential neighbourhood heating demand maximizing the use of solar energy and minimizing the network heat losses. Four modes of operation are planned considering the temperature levels of SDHS, which are enabled via on-off control switches. At the start:

1) In the first operational mode or DHW operation mode, the heat obtained by solar collectors is transported to the DHWT with the help of P_1, P_2, and P_5 pumps through HE_2. When the solar thermal energy is not enough to satisfy the demand in the DHW network, the auxiliary heater (AUX_2) is enabled. During DHW mode, the HP unit does not operate.
2) In the second mode, the SH gets initiated when a suitable level of temperature in DHWT (T_{DWT}) is reached while the temperature of the collector (T_{COL}) is at a higher temperature than the bottom of the SST (T_{SST}). In this mode of operation, P_1, P_2, P_3 pumps are used to transfer heat to SST from ST via HE_1.
3) In the third operation mode, a concurrent operation of DHW and SH circuits gets initiated when the criteria of DHW and SH operations are met and $T_{SST} > T_{DHWT}$.
4) In the fourth mode of operation, HP operates if the solar thermal system fails to satisfy the heating demand. Thus, in this mode of operation, the HP is activated when the $T_{COL} < T_{SST}$ which, subsequently is less than the reference turn-on temperature of the heat pump (T_{ref}). Under the HP operation mode, the heat generated is transported to either SST or DHWT depending on the demand. In this case, the uncovered heat demand is met by using the auxiliary heaters as well. In cooperation with the thermal SDHS part, the on-grid PV panels are integrated to reduce the purchased electricity from the supply grid while covering both the neighbourhood electric demand and SDHS electric equipment.

2.2. Simulation model

To model and analyze the SDHD system behaviour, TRNSYS 18 [53] has been used. This software uses partial differential equations and input constraints as limits for mass and energy conservation with defined boundary conditions. Due to the intrinsic dynamic nature of the system, it offers a realistic simulation of hybrid SDHS [54]. In order to reduce the computational cost, the hybrid SDHS model has been simulated for three benchmarking operational years. The solution is then inferred over the project lifetime, assuming that weather data and demand profiles are constant over the project lifetime (40 years). The SDHS model validation is performed based on the implemented work by Abokersh et al. [20] and Tulus et al. [55], incorporating the hybrid solar circuits and their control schemes. The information flow diagram is shown in Fig. 2. (Type – inside TRNSYS GUI).

Each component has information boxes for component-specific parameters and input-output variables. Mainly the model includes the following types: flat plate solar collectors (Type 1a) with an optical efficiency of 0.817, heat loss coefficient of 2.205 $W/m^2 \cdot K$; PV panel (Type 190) with a module conversion efficiency of 0.186; water to the water heat pump (Type 927), this model is supplied with normalized data files containing the manufacturer's catalogue data (WSHP-PRC026G-TRANE) for the heat capacity and power consumption for various operating temperatures; fully stratified storage tanks (Type 4c) with heat loss coefficient of 0.3125 $W/m^2 \cdot K$ for the DHWT, whereas the SST heat loss coefficient is a function of the selected construction materials; counterflow heat exchangers (Type 5b) with overall heat transfer coefficient of 3.931 $kW/m^2 \cdot K$; and auxiliary heaters (Type 6) with an efficiency of 93%. The secondary units are: single speed centrifugal pumps (Type 3b), inlet and outlet pipe ducts (Type 709), three-way valves (Type 11 h), controlled flow diverters (Type 11f), tempering valves (Type 11b), soil temperature profile for the SST (Type 77), weather data (Type 15–3), time-dependent forcing functions for the heating and DHW demand profiles (Type 9c), and controllers (Type 2b).

The thermal performance of a fluid-filled sensible energy storage tanks (Type 4c), subject to thermal stratification, can be modeled by assuming that the tank consists of N ($N \leq 100$) fully mixed equal volume segments. The degree of stratification is determined by the value of N. If N is equal to 1, the storage tank is modeled as a fully mixed tank, and no stratification effects are

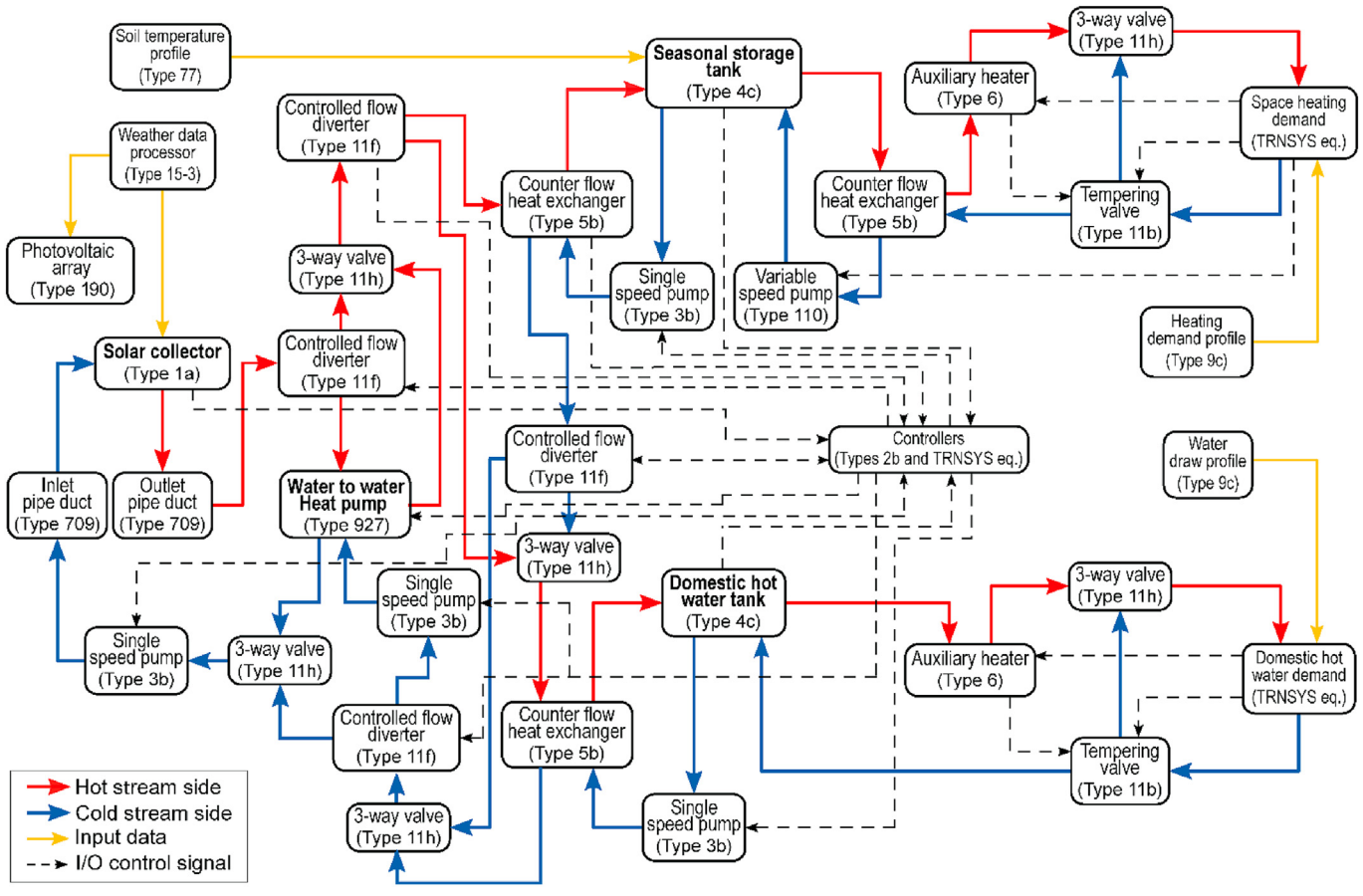

Fig. 2. Flow diagram of the SDHS system simulated, with the components and their interconnections used TRNSYS 18.

possible. At the current work, the storages are divided into 12 nodes for considering the stratification effect. This instance of Type 4 models a stratified tank having variable inlet positions such that entering fluid may be added to the tank at a temperature as nearly equal to its own temperature as possible. This instance further assumes that losses from each tank node are equal and does not compute losses to the gas flue of the auxiliary heater.

2.3. Decentralized reference case (base case)

In this setup, the heating demand (SH&DHW) of each building in the residential neighbourhood is satisfied through an individual air source heat pump (PUHZ-SW50VHA) with a coefficient of performance equal to 5 [21]. The heat pump compressor controller managed the required flow temperature based on the weather compensation routine and the zone setpoint (user adjusted). While the dwelling electric demand is met through the national grid. A schematic drawing for this decentralized system is shown in Fig. 3.

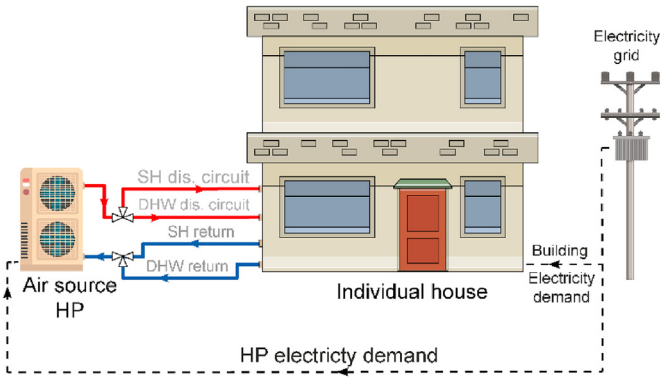

Fig. 3. Schematic drawing for the decentralized air source heat connected to the supply grid to cover an individual house demand.

2.4. The neighbourhood description and demand profiles

The neighbourhood consists of 10 newly retrofitted houses located in Emmen, Netherlands [21]. The dwelling layout is shown in Fig. 4, where each floor area is 60 m^2, and the ceiling height is 3 m. The considered dwelling has two external façades with a total area of 33.7 m^2, oriented to the East and West, whereas the opaque part represents 19.6 m^2. The outer walls of each dwelling are made of two primary walls, which are made using hollow bricks coated with plaster and insulation layers. The interior partition walls, made of gypsum boards, are finished with light concrete. The floor is made of two surfaces; the main ground surface comprises layers of insulation material, concrete, and stones, whereas the ground floor's inward surface is made of light concrete with gypsum boards. Moreover, the top roof surface composed of multiple layers of light concrete and plaster with insulation. A summary of the construction material properties is shown in Table 1.

To obtain real-time weather data for the dwelling, the climate data are obtained from a KNMI (Royal Netherlands Meteorological Institute) weather station. The nearest KNMI weather station to the dwellings in Emmen is in the Hoogeveen (STN:279,

Fig. 4. General view for the Emmen dwelling.

Table 1
Thermal properties of the building envelopes [56].

Parameter name	Unit	Value
Thermal resistance of the roof (RC_{roof})	[m^2K/W]	5
Thermal resistance of the floor (RC_{floor})	[m^2K/W]	5
Thermal resistance of the façade (RC_{facade})	[m^2K/W]	4.7
U-value of windows (U_{glass})	[W/m^2K]	1.1
Windows solar energy transmittance(G_{value})	–	0.7

LON(east):6.574, LAT(north):52.750, ALT(m):15.80), which is approximately 25–30 km away from the dwellings. The solar radiation in Emmen (Netherlands) varies from 23 kWh/m^2 in December to 155 kWh/m^2 in May. In summer (May–August), the solar radiation is towards the upper range of solar irradiance range. The heating and electricity demands are extracted from the hourly TNO measurements for these dwellings [56]. The buildings are heated up through radiators on all levels that are primarily provided by an air source heat pump (PUHZ-SW50VHA) at each building. The heat pump compressor controller managed the required flow rate based on the thermostats and the zone setpoint (user adjusted). Therefore, a variation in the heat pump performance factor (COP) is recognized with the variation in the ambient air temperature. Base on the time-dependent of the COP and its relative heat pump electricity consumption, the thermal heat pump power is estimated.

The thermal demand of the neighbourhood consists of an annual DHW demand of 5.29 MWh/house, and SH demand of 4.14 MWh/house. Apart from the heat demand, the annual electricity demand (5.53 MWh/house) is currently supported by the electricity grid. The total energy demand and its monthly variation for the dwelling are plotted in Fig. 5 alongside with monthly solar radiation and average monthly ambient temperature. DHW and electricity demand is decreased in the months of summer due to reduced activities of occupants in these months, while the space heating demand is significantly higher in winter due to low ambient temperatures and increased indoor occupant hours. Energy demand profiles (heat demand load for SH, DHW, and demand load for electricity) are provided as inputs variables for the time-dependent simulations of entire cases.

3. SDHS sustainability assessment

In the context of NZEB, the developed framework assesses proposed SHDS based on four main criteria: energy performance based on established energy efficiency indicators for the dwelling, the social indicator for direct and indirect benefits of society, economic performance and environmental impact throughout the system lifespan.

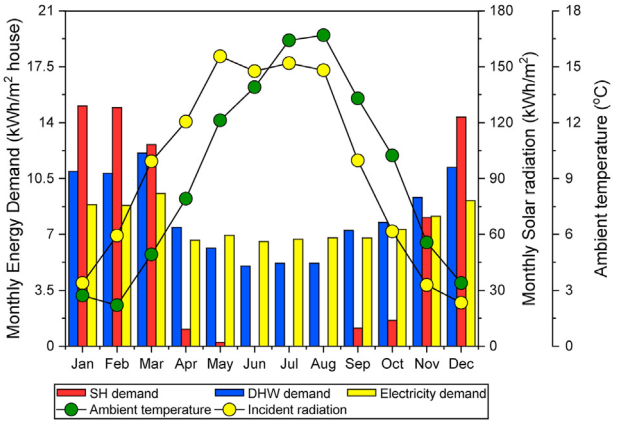

Fig. 5. Monthly average energy demand profile, solar radiation profile and ambient temperature profile.

3.1. Energy indicators

The SDHS energy performance is evaluated through a couple of indicators to evaluate both its thermal and electric renewable energy equipment.

Firstly, the REF_{th} is the renewable energy fraction calculated for the on-site utilization of solar thermal energy for SH and DHW demand. It can be defined as shown in eq. (1) [20].

$$REF_{th} = 1 - \left(R_{HP} + R_{fuel}\right) \tag{1}$$

where:

$$R_{HP} = \frac{\int_0^t Cap_{heating}}{Q_{SH\ load} + Q_{DHW\ load}} \tag{1.1}$$

$$R_{fuel} = \frac{\int_0^t \dot{Q}_{AUX_1} + \int_0^t \dot{Q}_{AUX_2}}{Q_{SH\ load} + Q_{DHW\ load}} \tag{1.2}$$

where $Cap_{heating}$ is the energy supplied by the heat pump. While $\dot{Q}_{AUX_1}$ and $\dot{Q}_{AUX_2}$ are the energy provided by the auxiliary heaters to cover the SH load ($Q_{SH\ load}$) and DHW load ($Q_{DHW\ load}$) under the condition of insufficient solar energy.

In addition, solar electric energy is evaluated through the REF_{elec} which represent the energy fraction calculated for the on-site utilization of renewable electrical energy to satisfy the electricity demand of the neighbourhood, and it is calculated as follows:

$$REF_{elec} = \frac{\int_0^t EC_{RE}}{Q_{electric\ load}} \tag{2}$$

where EC_{RE} is the generated electricity by the PV array, and $Q_{electric\ load}$ is the total electricity demand.

Since the SST usually presents a significant importance in the SDHS performance [2], the SST performance should be taken into account through, and its efficiency is calculated as follows.

$$\eta_{SST} = 1 - \frac{\int_0^t \dot{Q}_{SST\ loss}}{\int_0^t \dot{Q}_{HE_1}} \tag{3}$$

Where the $\dot{Q}_{SSTloss}$ is the heat loss through the SST and $\dot{Q}_{HE_1}$ is the heat transfer through the HE1.

Furthermore, the SST performance depends greatly on the amount of heat losses through the top, sideways and bottom of the storage. Therefore, Eqs. (4)–(6) are used to estimate the heat loss coefficients of the SST, as suggested by Hadorn [57].

$$U_{Roof} = \frac{1}{\frac{d_{con}}{\lambda_{con}} + \frac{d_{Roof}}{\lambda_{ins}} + \frac{1}{h_{conv}}} \tag{4}$$

$$U_{Wall} = \frac{1}{\frac{d_{con}}{\lambda_{con}} + \frac{d_{Wall}}{\lambda_{ins}} + \frac{1}{h_{conv}}} \tag{5}$$

$$U_{Gnd} = \frac{2}{R^2}\left\{ a\left(\frac{\lambda_G}{\pi}\right)^2 .\ln\left[\frac{a}{a - \left(\frac{\pi R}{\lambda_G}\right)}\right] - \frac{R.\lambda_G}{\pi} \right\} \tag{6}$$

Where:

$$a = \frac{\pi R}{\lambda_G} + \frac{(d_{con} + d_{Gnd})}{\lambda_G} + \frac{d_{con}}{\lambda_{con}} + \frac{d_{Gnd}}{\lambda_{Gnd}}$$

In these above equations U_{Roof}, U_{Wall} , and U_{Gnd} are the relative heat loss coefficients of the top, wall, and bottom of the SST. R is the SST radius, d_{con} represents the construction material thickness, whereas, d_{Roof}, d_{Wall} and d_{Gnd} represent the top, wall, and bottom surfaces insulation thicknesses of the SST, respectively. In addition, λ_{con} represents the thermal conductivity of the construction material, $\lambda_{ins}$and λ_{Gnd} represent the thermal conductivity of the insulating materials used for the roof, wall, and bottom surfaces of the SST, respectively. Parameter h_{conv} is the convective heat transfer coefficient to the air, and it is assumed to be 10 W/(m^2·K) for equations (4)–(6) [58]. The thermal conductivity of the ground λ_G is considered to be 3 W/(m·K).

Besides evaluating the SDHS performance, it is important to assess the effect of the proposed SDHS to enhance the building energy performance to achieve a nearly zero energy consumption at both scales: individual buildings and community. In this context, Energy Performance Indicators (EPI) present an estimation for the energy performance of the building. This index is widely used in the Netherlands as '*Dutch energy label for dwellings*' [22], and it is calculated as:

$$EPI = \frac{Q_{total}}{155A_{floor} + 106A_{loss} + 9560} \tag{7}$$

Where:

$$Q_{total} = Q_{SH\ load} + Q_{DHW\ load} + Q_{AUX} + Q_{electric\ load} - \int_0^t EC_{RE} - \int_0^t EG_S \tag{8}$$

where Q_{total} is the total energy consumption in the building, whereas EG_S is the generated thermal energy covered by the solar thermal energy system and A_{loss} is the area which is not heated up in the dwelling. The values obtained from eq. (7) are categorized corresponding to Dutch energy labels (from G to A++), as shown in Table 2, where the lowest Value of EPI indicates the highest building energy efficiency.

3.2. Economic indicators

The net present cost (*NPC*) assess the life cycle cost (LCC) to evaluate the SDHS feasibility over the project lifespan [58]. The *NPC* is calculated as a summation of the capital cost (*IC*), the operational cost (*OC*), and the replacement cost (*RC*). A detailed description of *NPC* calculation is provided in the supplementary information - SI 1.

$$NPC = IC + OC + RC \tag{9}$$

A common alternative approach to evaluate the economic feasibility is the payback period (*PBT*) which is the payback time of the proposed SDHS model [59], and it denotes the number of years taken by the proposed system to deliver the total life cycle cost [58].

Table 2
Dutch energy labelling for building's energy performance in 2013.

EPI	A++	A+	A	B	C	D	E	F	G
	<0.50	0.51–0.70	0.71–1.05	1.06–1.30	1.31–1.60	1.61–2.00	2.01–2.40	2.40–2.90	>2.90

It is calculated as:

$$PBT = \frac{NPC}{Annual\ cost\ saving} \tag{10}$$

3.3. Environmental indicators

The impact on environment of adding HP, SST and PV to the SDHS system is determined using the life cycle approach (LCA) [60]. LCA can be performed using a variety of indicators to determine the environmental impact of any technology. For the developed SDHS system, we use the ReCiPe 2016 [61] framework to determine the environmental impact. The ReCiPe is among the widely used environmental indicator due to the methodological perspective [62]. To calculate ReCiPe, Life Cycle Inventory Analysis (LCIA) data is transformed into endpoint scores, which are then categorized into three classes: human health, ecological systems, and resources depletion. Furthermore, theses damage classes are combined as a normalized indicator metric (*RCP*) for the SDHS conformation. The *RCP* can be expressed as:

$$RCP = \sum_{d} \delta_d \varepsilon_d DAM_d \quad \forall d \tag{11}$$

where DAM_d is the endpoint score for damage category *d*. $\delta_d$is a factor based on the use of extraction of material and use of land in the European setting to normalize endpoint data for different damage categories while ε_d is the weight factor based on values recommended in the ReCiPe 2016 framework. The data and environmental impact of SDHS components can be found in SI 2.

In addition, the environmental payback period (EPBP) is introduced to estimate the sustainability of the proposed SDHS model [20]. This indicator is estimated through calculating the total number of years required by the SDSH to replace the conventional system using the HP.

$$EPBP = \frac{RCP}{Annual\ RCP\ saving} \tag{12}$$

3.4. Social indicators

The proposed SDHS framework with the integration of multiple renewable energy technologies has a greater potential for providing social benefits, improving the quality of life of the residents in the dwellings, providing more and better employment opportunities (*EO*). This value can be estimated as [63]:

$$EO = \lambda_{E,grid} E_{nom} + \lambda_{heat} Q_{nom,heat} + \lambda_{PV} Q_{nom,PV} \tag{13}$$

Here $\lambda_{E,grid} = 0.61$ persons/MW is the grid electricity coefficient, $\lambda_{heat} = 0.38$ persons/MW is the solar thermal collector coefficient, and $\lambda_{PV} = 0.70$ persons/MW is the PV module coefficient; all of them used to calculate the employment coefficients for technologies incorporated in the SDHS system [64]. E_{nom}, $Q_{nom,heat}$, and $Q_{nom,PV}$ are nominal capacities of the power plant, roof mounted solar thermal collectors and roof mounted PV module, respectively [63].

4. Multi-objective optimization based on a surrogate model

Our objective is to enhance the economic and environmental performance of the proposed SDHS system. We used a surrogate modelling approach to implement multi-objective optimization on the SDHS system. The objective function is to minimize the net present cost and the environmental impact of a SDHS for a residential community while tracking its technical and social performance. In this work, we used surrogate models, which uses simulation results obtained with the TRNSYS model validated in section 3 to train a neural network to predict the thermal performance of the SDHS. Running the SDHS TRNSYS model with a feasible range of decision variables provides a set of feasible scenarios used as a training data set for the ANN. The trained ANN is then coupled to a genetic algorithm to devise a multi-objective optimization (MOO) function for minimizing *NPC* and *RCP* under several technical constraints.

4.1. Data generation

Dataset development is a key aspect when developing a surrogate model, as a valid dataset obtained from a large number of simulations is used to train the surrogate model. For this work, data generation is performed by identifying the uncertain independent variables (inputs) and providing them to the TRNSYS simulation tool to obtain the dependent variables (outputs). In this work, the independent variables comprising the performance of the solar circuit, the SH distribution circuit and the DHW distribution circuit are used to create a combination of inputs to obtain the sample point. More details regarding the data generation are introduced in Abokersh et al. [20].

4.2. Surrogate model convergence

The metamodel is built based on a multi-layer feedforward ANN model, where this model contains 14 neurons in the input layer and three hidden layers. The ANN simulations are implemented based on the Bayesian regularization algorithm with a learning rate and a Momentum mean of 0.001 and 0.004. The model structure is determined through the optimization approach proposed by Abokersh et al. [58] to provide a relatively good convergence. In the ANN model, 21 outputs are considered in the output layer. These outputs include the energy produced in the solar collector field, the energy supplied by the heat pumps, the energy supplied by the storage tanks, and energy covered by the auxiliary heaters. The metamodel is validated using the performance metrics: (i) adjusted R^2 ($R^2-adj.$) and (ii) variation coefficient (*CV*). Equations (14)–(16) shows the mathematical form of $R^2-adj$and *CV*.

$$R^2 = 1 - \frac{\sum_{i=1}^{n} \left(y_{predict,i} - y_{data,i}\right)^2}{\sum_{i=1}^{n} \left(y_{data,i} - \overline{y}_{data}\right)^2} \tag{14}$$

$$R^2 - Adj. = 1 - \frac{\left(1 - R^2\right)(n-1)}{n-k-1} \tag{15}$$

$$C.V(\%) = \sqrt{\frac{\sum_{i=1}^{n}\left(y_{predict,i} - y_{data,i}\right)^2}{\overline{y}_{data}}} \times 100 \tag{16}$$

Here, $y_{predict,i}$ represents the value estimated at a time 'i', $y_{data,i}$ shows the value of output y at a time 'i', n displays the sample size while k shows the total number of regressors used.

4.3. Optimization algorithm and surrogate model integration

After developing the surrogate model, the next step is to incorporate the heuristic optimization techniques with the robust ANN model to solve a MOO problem. MOO framework deals with two or more conflicting objectives in the objective function. In this case study, the energy performance of the system is optimized by adjoining the environmental and economic system requirements. Ultimately, the residential community size's impact is also examined on the SDHS performance in an extended optimization problem. For the proposed SDHS system, the objective function to simultaneously optimize the *NPC* and *RCP* is given as:

$$\begin{aligned} &min\{f_1(x), f_2(x)\} \\ &s.t.\ h(x) = 0 \quad g(x) \geq 0 \\ &lb_i \leq x_i \leq ub_i \quad i \in \{1, \ldots, 18\} \end{aligned} \tag{17}$$

Here, f_1 is *NPC*, f_2 is *RCP*, h represents equality constraints corresponding to the physics of physical systems solved in TRNSYS, and g denotes inequality constraints corresponding to technical evaluation of SDHS. These constraints must maintain the annual solar collector efficiency above 60%, whereas SH annual solar fraction and SST efficiency should be maintained above 50% as recommended by Bauer et al. [65] and Solites [66].

The solutions of multi-objective functions provide us with a non-dominated solution called Pareto solutions, which represent the optimal trade-off for the economic and environmental targets. To avoid obtaining sub-optimal solutions (which is probable in classical MOO using point by point search), an improved technique called Pareto-ranking [67] is utilized to refine the solutions for *NPC* and *RCP*. The simulation-based optimization model is obtained by merging the generated robust metamodel based on ANN and the NSGA-II algorithm. Based on Alajmi et al. [68] recommendation, the multi-objective genetic algorithm (MOGA) uses the NSGA-II algorithm with 1000 preliminary population due for 300 generations.

The performance for SDHS has been examined for various community sizes (10, 25, 50, 100, and 500 houses) based on the decision variables explained in ensuing section.

4.4. Decision variables and parameters

In the case study, 18 decision variables are used to formulate an optimization problem, including system components' relative alignment, structure, operating criteria and sizing. To categorize these variables, decision variables are classified into 3 field circuits, namely (i) supply (ii) SH (iii) DHW (Fig. 6). These decision variables are linked with mathematical equations to determine the equipment size for SDHS. The solar field circuit has 5 decision variables, i.e., the area of photovoltaic panels (A_{PV}), area of the solar thermal collector (A_{col}), the inclination angle of solar collectors, including the photovoltaic and thermal collectors (β_{col}), number of solar thermal collectors in series (N_{col}), heat pump capacity as a function of the maximum heat demand supplied (FC_{HP}), the turn-on

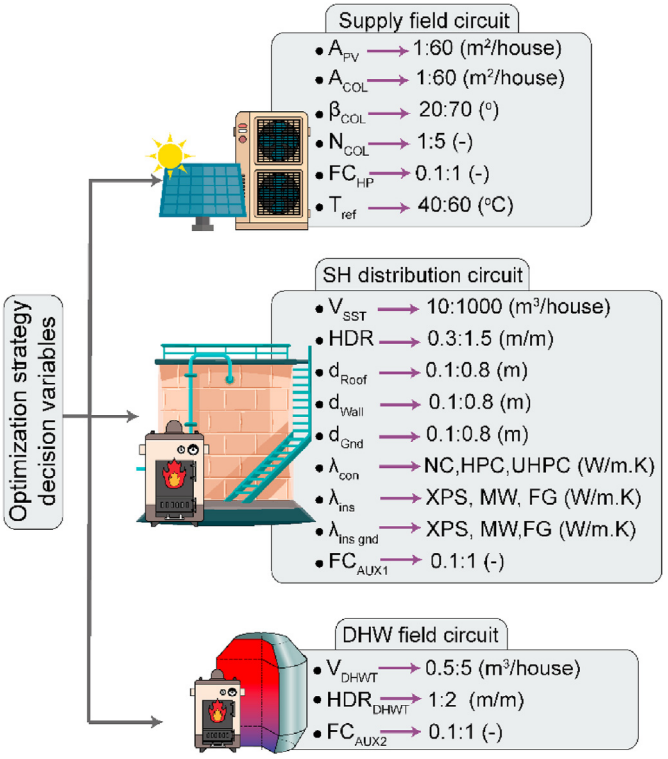

Fig. 6. Classification of the decision variables in the SDHS optimization problem.

temperature of the heat pump (T_{ref}). The space heating circuit has 9 decision variables, i.e., the volume of SST (V_{SST}), height to diameter ratio for SST (HDR), the thickness of insulation for the wall (d_{wall}), roof (d_{roof}), and ground (d_{Gnd}), insulation material type represented by the conductivity of construction material (λ_{con}), roof and wall (λ_{ins}) and ground ($\lambda_{ins,gnd}$), and auxiliary heating unit capacity as a fraction of the maximum heating demand (FC_{AUX_1}). Finally, the domestic hot water circuit has 3 decision variables, e.g. volume of DHWT (V_{DHW}), height to diameter ratio of DHWT (HDR_{DHWT}) and the fraction capacity supplied by the auxiliary unit as a percentage of the maximum heating load (FC_{AUX_2}).

5. Optimal solutions post analysis

We have proposed a framework for the inclusive sustainability assessment of a solar assisted district heating system. The methodology is outlined in Fig. 7. The framework starts with the simulation of SDHS in TRNSYS 18 and defines the most suited decision variables, their range and related output to showcase the thermal performance of the SDHS. To reduce the computational cost of the process, the TRNSYS model is coupled with MATLAB and an ANN with Bayesian optimization. Later, the MOGA is coupled with the neural network to perform the multi-objective optimization for economic and environmental objectives. MOO provides a Pareto frontier with the optimal solutions for different community sizes, which are then subjected to multi-criteria decision making (MCDM) to facilitate the selection according to the needs/preferences of stakeholders. For MCDM, we used Technique for Order of Preference by Similarity to Ideal Solution (TOPSIS), which ranks the solutions based on the desired criteria. To illustrate the significance of uncertainty on the optimized objectives, we performed a global sensitivity analysis (GSA) [69].

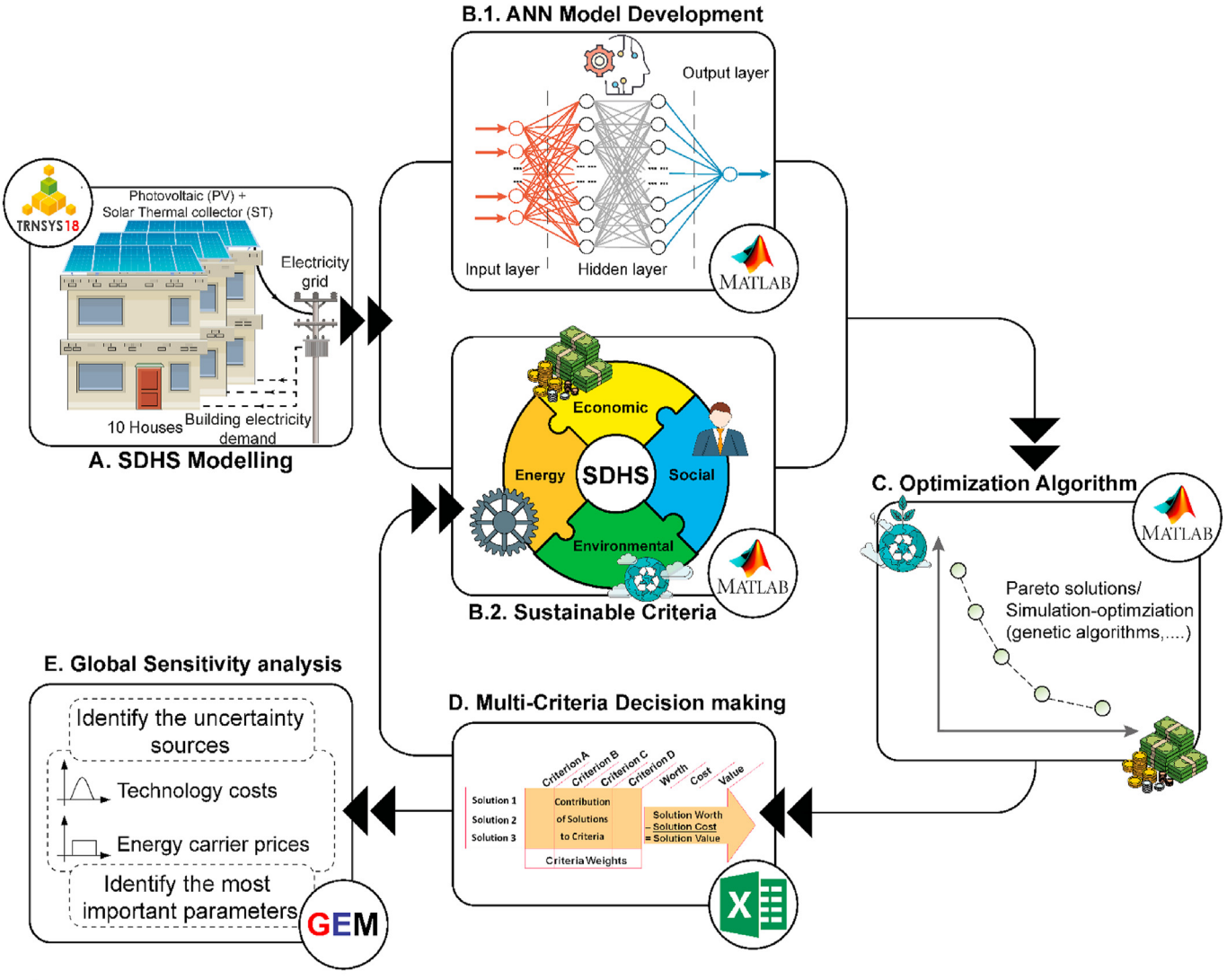

Fig. 7. Framework for the hybrid multi-objective optimization system of SDHS.

5.1. MCDM development for SDHS evaluation

5.1.1. Indicators normalization

The indicators used for the sustainability evaluation vary in nature and value range. Before applying the MCDM, we normalize the indicators to a common range [0,1]. We used a distance-based normalization (TOPSIS) for the MCDM [70]. The normalization method for the indicator being minimized is expressed in Eqs (18, 19), while for the indicator being maximized is expressed in Eqs. (20 - 21):

$$v_{ij} = \frac{x_j^{min}}{\overline{x}_{ij}} \tag{18}$$

$$x_j^{min} = min\left(\overrightarrow{x}_{ij}\right) \tag{19}$$

$$v_{ij} = \frac{\overrightarrow{x}_{ij}}{x_j^{max}} \tag{20}$$

$$x_j^{max} = \max\left(\overrightarrow{x}_{ij}\right) \tag{21}$$

5.1.2. Indicators' weighting method

The importance of each criterion might be different for each stakeholder. There are subjective and objective methodologies to apply weighting factors [71]: objective methods are based on mathematical models and more suited for numerical data. One of the widely used objectives is the entropy-based weighting approach, and it is easily adaptable [72]. Suppose, a set '*D*' which represent our sustainability criteria characterized by a vector $d_j = (d_{j_1}, d_{j_2}, \ldots, d_{j_m})$ in terms of normalized indicator '*i*' is defined as:

$$D_j = \sum_{i=1}^{m} d_{ij_j} = 1, 2, \ldots, m \tag{22}$$

Then, the entropy of j^{th} indicator is given by:

$$e_j = -\frac{1}{\ln(m)}\sum_{i=1}^{m}\frac{d_{ij}}{D_j}\ln\frac{d_{ij}}{D_j} \tag{23}$$

In the end, the normalized weight is calculated as:

$$w_j = \frac{1-e_j}{\sum_{j=1}^{m}(1-e_j)} \tag{24}$$

5.1.3. TOPSIS distance-based normalization method

The TOPSIS algorithm, developed by Hwang et al. [73], is widely used in MCDM problems. This method uses the normalized values obtained from Eqs (19-21) and assumes a distance-based criterion indicating that the ideal solution lies at the shortest distance from the positive ideal solution and the longest distance from the negative ideal solution. The calculated distances are then compared to find out the best plausible solution. The advantage of TOPSIS is that it can provide a ranking of each solution for each criterion [74].

To determine the rank, first, we identify the positive ideal solution (A^+) and the negative ideal solution (A^-):

$$A^+ = \left\{\left(\underbrace{max}_{i} v_{ij} \middle| j \in I\right), \left(\underbrace{min}_{i} v_{ij} \middle| j \in I'\right),\ i = 1,2,\ldots,m\right\} = \left\{v_1^+, v_2^+, \ldots, v_m^+\right\} \tag{25}$$

$$A^- = \left\{ \times \left(\underbrace{\min}_{\text{UnderBrace}\ i} v_{ij} \middle| j \in I\right), \left(\underbrace{\max}_{\text{UnderBrace}\ i} v_{ij} \middle| j \in I'\right),\ i = 1,2,\ldots,m\right\} = \left\{v_1^-, v_2^-, \ldots, v_m^-\right\} \tag{26}$$

Here, $I = \{j = 1, 2, \ldots, n\}$ and $I' = \{j = 1, 2, \ldots, n\}$ represent the sets of economic and environmental criterion. Then, we measure the Euclidean distance for each solution from the positive and negative ideal solutions using the following equations:

$$S_i^+ = \sqrt{\sum_{j=1}^{n}\left(v_{ij} - v_j^+\right)^2}, \quad for\ i = 1,2,\ldots,m \tag{27}$$

$$S_i^- = \sqrt{\sum_{j=1}^{n}\left(v_{ij} - v_j^-\right)^2}, \quad for\ i = 1,2,\ldots,m \tag{28}$$

Lastly, proximity index ($C_i \in [0,1]$ for $i = 1, 2, \ldots, m$) is calculated to find the remoteness from the positive and negative ideal solutions for ranking, as:

$$C_i = \frac{S_j^-}{S_j^+ + S_j^-} \tag{29}$$

5.2. Global sensitivity analysis (GSA)

The final step of this methodology is to perform a sensitivity analysis to offer an understanding of the most sensitive system parameters. Given GSA's advantage over LSA, a Bayesian-based GSA approach (BACCO) [75] is employed. This approach can cover an extensive range of parameters with an interaction for their relative distribution under uncertainty. It also reduces the computational time compared to Monte-Carlo based GSA approach.

BACCO methodology has two main stages: (i) acting as an emulator (statistical representative model) and (ii) uncertainty analysis. The emulator is trained with the data obtained from the simulation-optimization model. This dataset covers the feasible domain of solutions in a Latin hypercube design. Once the emulator is working, it is cross-validated to check its efficiency. The second stage covers the multidimensional domain of design variables to quantify the sensitivity of the parameters. The GSA is performed with respect to *EPI*, *NPC*, *RCP*, and *EO* in terms of percentage variation of each input to estimate the impact of ten economic decision variables. These variables comprise natural gas price (C_{ng}), buying (C_{el}) and selling to the grid electricity prices (S_{el}), natural gas (i_{ng}), electricity inflation rate (i_e), investment cost (*IC*), operational cost (*OC*), replacement cost (*RC*), in addition to system inflation (i) and discount rates (d). The performed sensitivity analysis is presented in terms of the percentage variance contribution (σ) of each input with respect to the (a) Energy indicator; (b) Economic indicator; (c) Environmental indicator; and (d) Social indicator.

6. Results and discussion

This work provides a sustainable insight into the applicability of surrogate models for the economic-environmental-social optimization of the transient SDHS model. The surrogate model was used to optimize the SDHS framework for different community sizes ranging from 10 to 500 houses under different scenarios (i.e., scenario 1: minimum cost; scenario 2: 25% less environmental damage; scenario 3: 50% less environmental damage; scenario 4: 75% less environmental damage; and scenario 5: minimum environmental damage). The wide range of the decision variables produced multiple results, which are discussed in the following sections. The first portion of the results and discussion section addresses the metamodel's fittingness for the SDHS framework optimization. The second portion sheds light on the SDHS optimization results for economic-environmental-social indicators and physical and technical constraints. In this section, optimal solutions are analyzed for all community sizes under each scenario. The third portion provides an insight into the ranking of the optimal solutions based on weighted criteria using multi-criteria-decision-making. The final portion checks the robustness of the metamodel using the global sensitivity analysis.

6.1. Surrogate model convergence results

In this work, a K-fold cross-validation strategy is adopted to fit the surrogate model. The 2048 samples (i.e., simulation results) are organized in k subsets [76]. The ANN model is trained with k-1 subsets, while kth subsets are used to test the trained model in each run. Table 3 displays a summary of the ANN model performance.

Results in Table 3 show that the surrogate metamodel prediction agrees with TRNSYS simulation outputs where *C.V* has good model accuracy (maximum deviation 8.87%) for any surrogate model output as the $R^2 - Adj.$ is always above 95.5% for all outputs. Hence, we can be confident about the ANN model's predictability for the proposed SDHS framework's thermal performance for the given training data range. Metamodeling offers significant reductions in computational time compared with conventional heuristic optimization techniques.

6.2. Multi-objective optimal solutions

The validated ANN-based surrogate model is employed to

Table 3
Performance of ANN model in predicting the TRNSYS simulation output.

	Solar circuit					SH circuit			DHW circuit		
	Q_{SOL}	Q_{PV}	Q_{Useful}	Q_{abs}	P_{elec}	Q_{SST}	$Q_{SST\ loss}$	Q_{AUX_1}	Q_{DHW}	$Q_{DHW\ loss}$	Q_{AUX_2}
R^2 – Adj.	99.8%	99.7%	98.3%	97.7%	97.8%	99.5%	97.7%	99.2%	95.5%	98.9%	99.4%
C.V	1.98%	1.87%	3.97%	8.87	8.16%	2.87%	8.54%	8.15%	0.49%	2.70%	3.08%

optimize the economic and environmental performance of the SDHS for various community sizes and under different scenarios (i.e., scenario 1 - minimum cost, scenario 2–25% less environmental damage, scenario 3–50% less environmental damage, scenario 4–75% less environmental damage and scenario 5 - minimum environmental damage). All the scenarios are compared to the base case (decentralized heat pump) explained in section 2. The first set of optimal results for the economic criteria are shown in Fig. 8. Economic criterion (*NPC*) is simplified to €/m^2 of the building. Base case has *NPC* at 66.6 €/m^2 which is constant for all the scenarios. For the smallest community size (10 houses), the optimal solution for scenario 1 (minimum cost) has an economic performance analogous to the base case (70.1 €/m^2). The economic performance for 10 houses community size decreases with the decrease in environmental damage factor of SDHS as the *NPC* for scenario 5 (minimum environmental damage) is 125 €/m^2. However, as the community sizes increase from 10 to 25, 50, 100 and 500 houses, the economic performance increases significantly and proportionally. For 25 houses community sizes, the economic performance is improved for scenarios 1, 2, 3 and 4 by 32%, 28%, 23% and 12%, respectively, over the base case. While scenario 5 has an unfavourable performance for 25 community size compared to the base case as the base case outperforms the former by 22%. For 50 houses community size, the optimal SDHS solution surpasses the base case's economic performance for scenario 5 (minimum environmental damage) and has an *NPC* of 64.7 €/m^2. For community sizes higher than 50 houses, the proposed SDHS has economic and environmental solutions over the base case for every scenario considered here. The best economic solution is obtained for the minimum cost scenario in 500 houses community (21 €/m^2). For scenario 4 and scenario 5, the economic performance is similar at a value of *NPC* equal to 30.7 €/m^2.

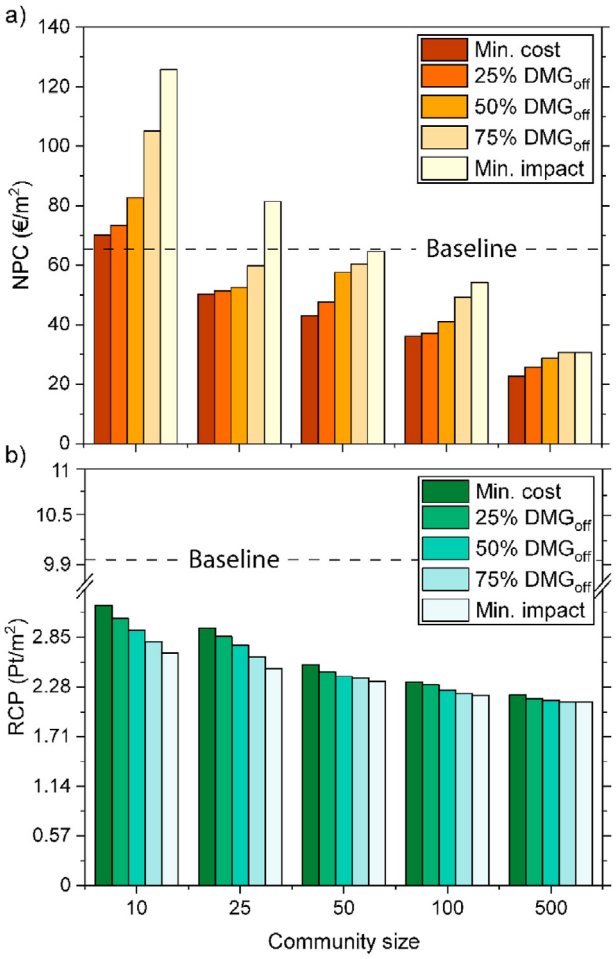

Fig. 8. Optimal solutions of SDHS for various community sizes under different scenarios where (a) the economic criteria, whereas (b) the environmental criteria.

The environmental damage factor (Fig. 8) shows that all optimal solutions have a better environmental performance compared to the base case, which has *RCP* value of 10.1 Pt/m^2 while the least environmental friendly optimal solution is the minimum cost (scenario 1) for 10 houses community size which has a *RCP* value 3.2 Pt/m^2, which improves by 300% the environmental performance compared with the base case. Therefore, all the optimal solutions perform extremely well for environmental criterion against the base case. Like the economic performance, the environmental performance of the SDHS improves as we move to bigger community sizes since it is possible to cover the energy demand by a higher percentage of renewable energy. The case of 500 houses community gives the best environmental performance for scenarios 4 and 5 with *RCP* value of 2.1 Pt/m^2 which shows an impressive 400% improvement compared with the base case's economic performance. Thus, the use of ANN model's enables to find optimal solutions which improved environmental and economic performance compared to the base case.

To arrive at the optimal solutions described above and depicted in Fig. 8, the metamodel considers multiple decision variables for different scenarios and community sizes. The optimal design and sizing of the SDHS also become an important consideration to achieve the desired economic and environmental performances. An in-depth analysis of the optimal solutions obtained provides us with a guideline for the SDHS system design and sizing. SDHS was divided into three circuits, namely: (i) Space heating circuit; (ii) Solar field circuit; and (iii) Domestic hot water circuit. Each circuit consists of specific components to serve specific purposes in the SDHS network. These decision variables vary due to multiple scenarios and provide a guideline for optimal system design. This range of the decision variables for optimal solutions is shown in Fig. 9. Each diagram has lower wick (representing minimum cost scenario), a center body (representing the scenario 2, 3 and 4) and the upper wick (representing minimum environmental damage scenario).

To facilitate a comprehensive sustainable analysis of the optimal SDHS solutions, a breakdown of the key performance indicators mentioned in section 3 is shown in Fig. 10. The performance indicators are divided into 4 main categories: (i) Energy; (ii)

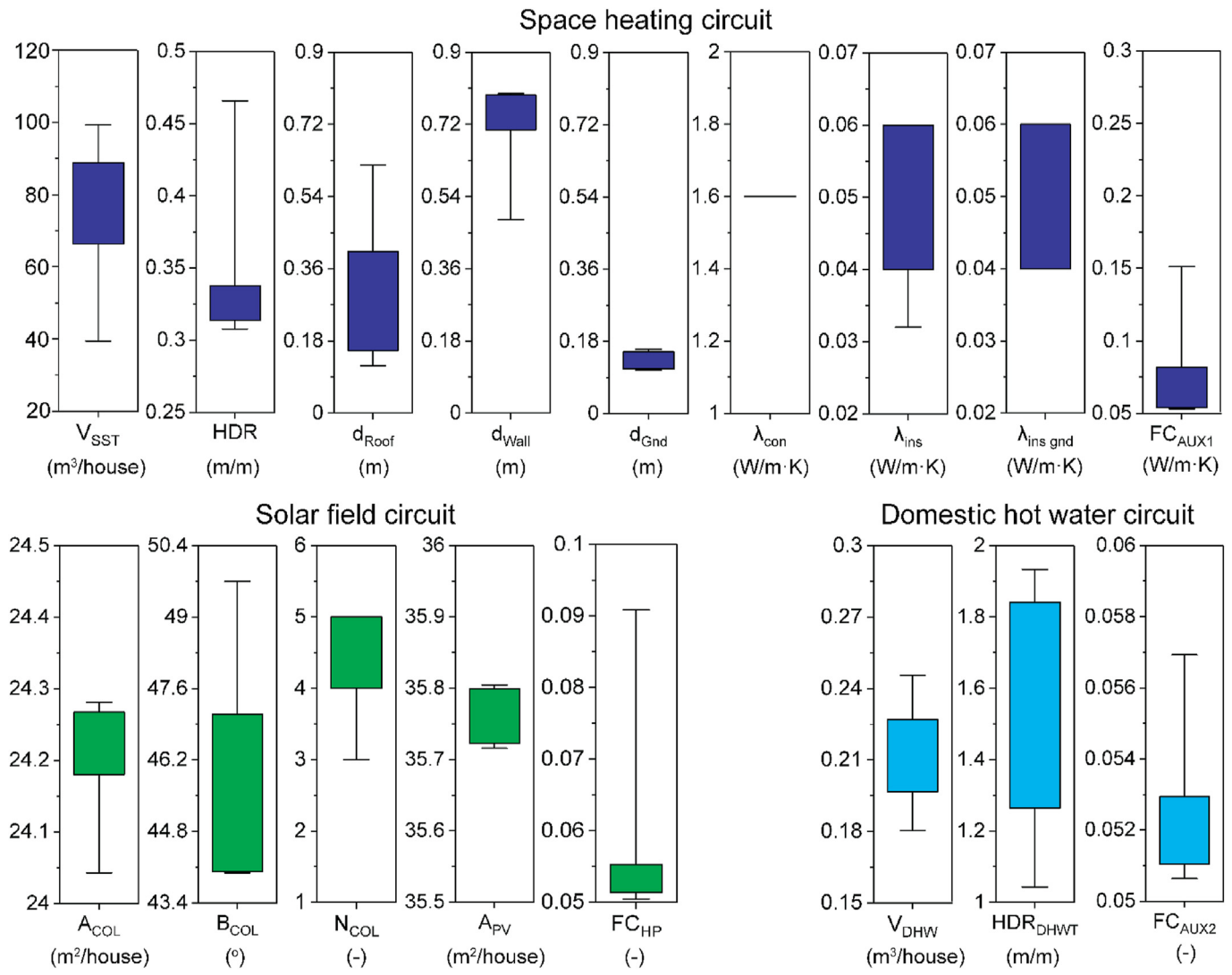

Fig. 9. Guideline for key parameters values to design optimal SDHS solution under various scenarios.

Economical; (iii) Environmental; and (iv) Social. All scenario solutions perform better for the smallest community size of 10 houses than the base case for energy indicators. The performance of energy indicators improves from minimum cost scenario to minimize environmental damage scenario in general for all the community sizes, although the gradient for improvement from scenario 1 to scenario 5 is high for 10 houses community size. A comparison between scenario 1 and the base case for 10 houses shows 2.5 folds improved EPI performance (building energy performance grade = A+) for the optimal solution against the base case (building energy performance grade = D). In contrast, the optimal solution of scenario 5 has 4 times improved EPI performance over the base case to achieve a building energy performance grade A++. For social indicator, the 10-houses community size has 350% improved performance for all the scenarios. As we move towards bigger community sizes, EPI's performance increases from 0.56 to 0.16, giving us a significant improvement range from 3 to 10 times in the energy performance over the base case for different scenarios. The building energy performance is reflected by the solar thermal fraction, which can increase from 81% on a community of 10 houses up to 95% on a community size of 500 houses. On the other hand, the installed PV system provides extra electricity of around 70% for all community sizes to be sold to the electricity grid, which can support the PEB state. Furthermore, the increment in solar energy usage with increasing the community size is reflected in the reduction of natural gas usage where it diminishes from 23% at the scenario 1 community size of 10 houses to only 5.6% under the same scenario at community size of 500 houses.

For economic indicators, optimal solutions have a better scope in the long term because of the PBT indicator. In contrast, the base case is depreciative and has no payback, while optimal solutions have a payback and, therefore, provide a better option for long term planning. However, as we move to bigger community sizes, from 25 to 500 houses, economic indicators overcome the base case, and we find that for 50 houses community size, even the most environment-friendly solution has better economic performance than that of the base case with the payback period of 26 years. Furthermore, with the movement toward a bigger community size of 500, the PBT can be reduced to 13.6 years. The environmental indicator has shown an improved performance for all the community sizes under all scenarios, where the environmental performance is improved from 11.7 years at community size of 10 houses to 8.4 years at community size of 500 houses. Similarly, the social indicator shows improved performance for the optimal

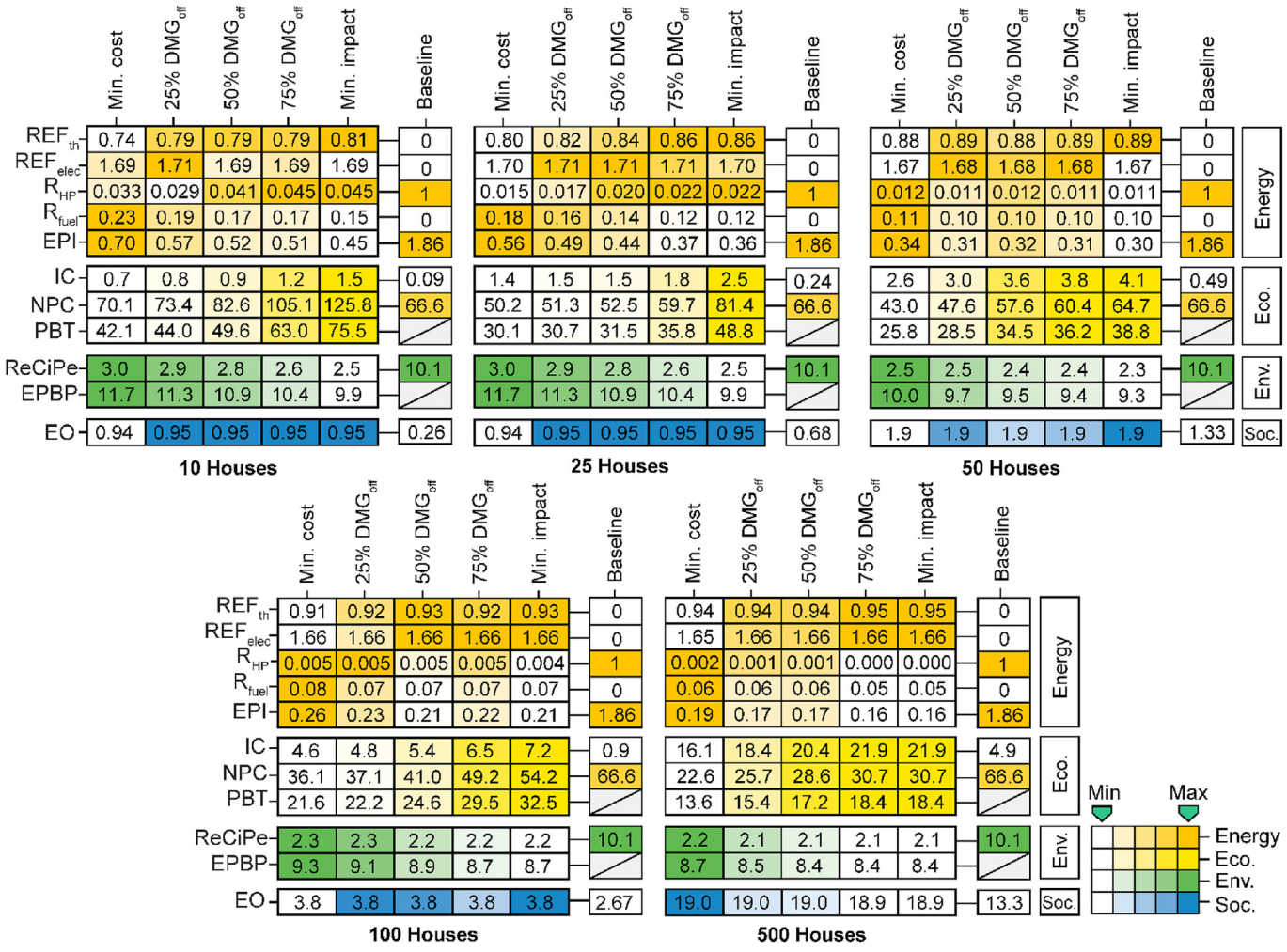

Fig. 10. Key performance indicators for best ranked optimal solutions and base cases under different community sizes.

solutions over the base case, ranging from 1.3 times for 10 houses community size to 4 folds for 500 houses community size.

6.3. Optimal solutions ranking based on MCDM

The large set of optimal solutions obtained from the ANN model under different scenarios for different community sizes provide stakeholders with multiple options to choose from. To facilitate the stakeholders' decision-making, a ranking system is developed using multi-criteria decision making (MCDM). The criteria considered for this ranking system are energy, economic, environmental, social and a hybrid considering all the criteria. A summary of the indicators used for each criterion alongside their weight is shown in Table 4. A weighted entropy TOPSIS approach described in section 5.1 is used to rank the solutions under various scenarios.

The ranking of optimal solutions for different community sizes under the considered five scenarios is shown in Table 5. The balance scenario (i.e., 50% DMG_{off}) gets priority for 10, 25 and 100 houses community size while it turns out 2nd ranked for 50 houses community and 3rd for 500 houses community. For 50 houses community size 25% DMG_{off} is best ranked while for 500 houses community 75% DMG_{off} is the first solution. It is worth noting that in 500 houses community, more environment-friendly solutions (i.e., scenario 4 and 5) make the top ranks by a clear margin and stand out.

6.3.1. Technical analysis

To analyze optimal solutions' thermal and energy performance, the technical analysis has been performed for optimal solutions. The thermal energy is used for space heating and hot water

Table 4
Weighted indicators to apply TOPSIS for MCDM.

	Indicators	Weights
Energy	($W_{REF_{th}}$, $W_{REF_{elec}}$, $W_{R_{HP}}$, $W_{R_{fuel}}$, W_{EPI})	(1.2%, 0%, 38.2%, 30.3%, 30.3%)
Economic	(W_{IC}, W_{NPC}, W_{PBT})	(43%, 28.5%, 28.5%)
Environmental	(W_{ReCiPe}, W_{ADSR})	(50%, 50%)
Social	(W_{EO})	(100%)
Hybrid system	(W_{Energy}, $W_{Economic}$, $W_{Environmental}$, W_{Social})	(28.8%, 67.8%, 3.2%, 0.2%)

Table 5
Ranking of optimal solutions based on community size and scenario.

Community size	10 houses		25 houses		50 houses		100 houses		500 houses	
Scenario	P_i	Rank	P_i	Rank	P_i	Rank	P_i	Rank	P_i	Rank
Min. cost	0.73	3	0.71	4	0.77	3	0.76	3	0.64	5
25% DMG_{off}	0.75	2	0.73	3	0.80	1	0.77	2	0.71	4
50% DMG_{off}	0.76	1	0.76	1	0.77	2	0.79	1	0.73	3
75% DMG_{off}	0.70	4	0.75	2	0.75	4	0.75	4	1.00	1
Min. impact	0.65	5	0.65	5	0.72	5	0.71	5	0.99	2

demands. As shown in Fig. 11, the plots depict the energy demand and energy supplied (Q_{cov}) by the solar collectors (thermal and PV) for all the community sizes throughout the year. Space heating demand (kWh/m^2) is high for the winter months (November, December, January and February). For November, December, and January, the proposed SDHS system can provide 100% of the thermal energy to satisfy the demand in every community size. The SH demand is not met by Q_{cov} in the months of February and March for 10, 25 and 50 houses communities and the excess demand in these cases is satisfied by the auxiliary unit. The plot also shows that as the community size increases the Q_{cov} is able to cover more SH demand and for community size of 100 houses and above, the SDHS can satisfy SH demand fully on its suggesting of reduction in environmental damage at the SDHS for bigger community sizes.

The DHW demand exists throughout the year, unlike SH demand. The DHW demand has 20%–50% increase in the months of winter and Q_{cov} needs to be supplemented with auxiliary units to meet this extra demand for DHW. Q_{cov} shows a very small increasing gradient with the increase in community sizes, as shown in Fig. 11. The electricity demand also has a similar nature as the SH and DHW demand over the year. Electricity demand is higher in October–March than the EC_{RE} produced by PV panels for the all the community sizes. Therefore, the excess electricity demand is met by grid electricity through smart metering. In April–August, PV collectors' electricity is higher than the demand. This extra production of electricity is supplied to the grid through smart metering to earn credits. These results show the transition not only to the NZEB concept, but it can serve the transformation from LCB to PEB for community sizes with more than 100 houses.

6.3.2. Economic analysis

The economic performance of optimal solutions is further analyzed by breaking down the *NPC* into its various components. Fig. 12 shows the cost distribution of SDHS components for the top-

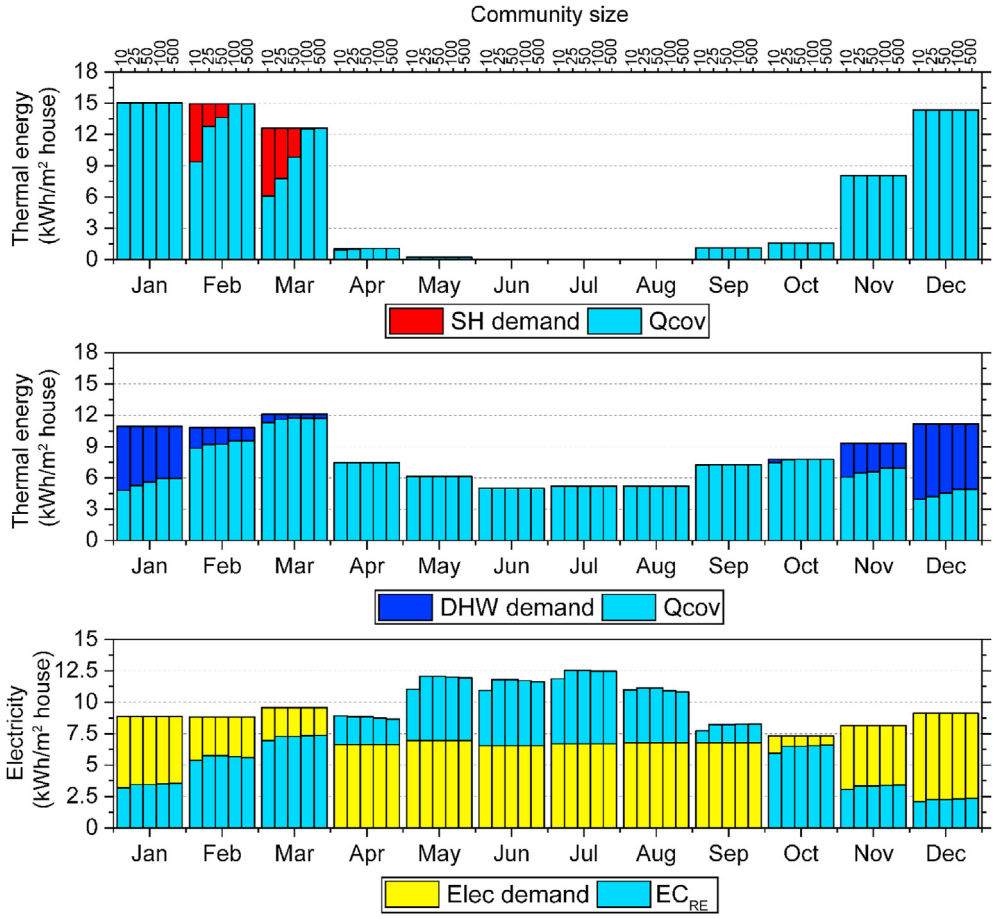

Fig. 11. Energy demand and supply (per m^2) for all community sizes throughout the year. The figure consist of two layers where the demand profiles are plots in the back layer, whereas the renewable coverages are plotted at the front layer.

ranked solutions for every community size, mentioned in section 6.2, the analysis of the cost components for the base case has a very low capital cost (6.2%) and replacement cost (7.8%) while the operational cost is extremely high (86%) which makes the base case a depreciating project as each operational costs adds to the cost of the project. On the other hand, for optimal solutions, the project's capital cost varies from 46.6% to 56.1%, operational cost varies from 13.2% to 1.6%, and replacement cost varies from 40.4% to 42.3%. The capital cost percentage of the optimal solutions increases as the community size increases because bigger community sizes corresponding to scenario 4 and scenario 5 (less environmental damage) have more renewable energy technology and a high capital cost. The operational cost of the SDHS system reduces as we approach bigger community sizes, while the SDHS solution also provides more than 40% of the *NPC* as replacement costs which suggest that the depreciation of the SDHS project is reduced by at least 500%. Finally, with the increment in the community size, the total SDHS cost dramatically increases, especially moving toward more green solutions requiring extra investments. Thus, the SDHS for the community of 10 houses has a total life cost of €1.98 M, and it increases up to €36.8 M for the community size of 500 houses.

6.3.3. Environmental analysis

The environmental indicator is an important part of this study. Therefore, a detailed analysis of optimal SDHS solutions is performed to see each ranked optimal solution environmental impact. Fig. 13 shows the distribution of environmental damage caused by each component of the SDHS solutions compared to the base case below for the same community size. *RCP* points measure the environmental damage of each component. For the base case, the main cause of environmental damage is the electricity consumption from the grid. For 10 houses and 100 houses community sizes, under 50% DMG_{off} scenario, the environmental damage is almost 10 times lower than for the corresponding base cases while it is comparable for 25 houses community size under the same scenario. For 25% DMG_{off} and 75% DMG_{off} scenario, environmental damage is more than 10 times lower compared to the base cases for corresponding community sizes.

Component wise environmental analysis of SDHS solutions provides us with a better understanding of the damage caused by each system. Fig. 13 entails that as we increase the community size, environmental damage due to the consumption of natural gas reduces significantly; for example, in the optimal SDHS system for 10 houses, the environmental damage caused by natural gas consumption is 38% of the total damage while that in case of 500 houses is just 17%. The percentage of environmental damage due to solar collectors (PV + thermal) is the major constituent (49%–67%) for environmental impact for all SDHS solutions. A third major

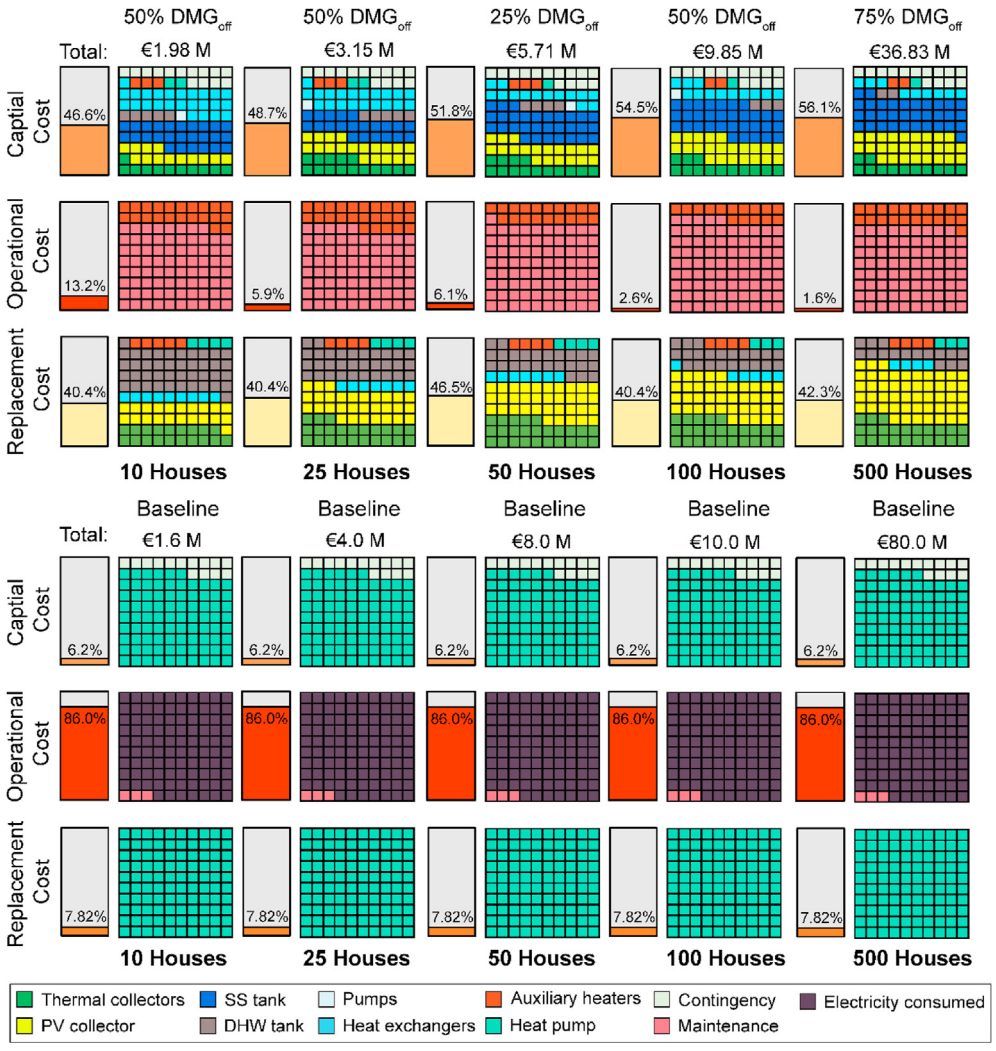

Fig. 12. Cost analysis of optimal solutions for different community sizes compared to base case for respective community sizes.

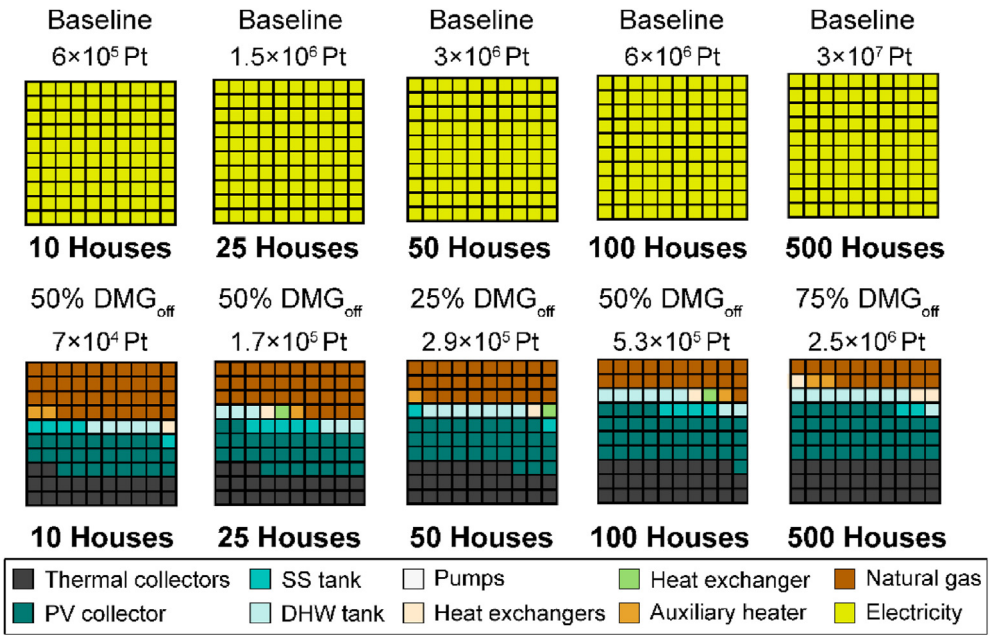

Fig. 13. Comparison of results of environmental analysis under different optimal scenarios for various community sizes.

contributor to environmental damage in optimal solutions is SST, which constitutes 4%–6% of total damage. Other components for environmental damage are auxiliary units (1%–2%), heat exchangers (2%), DHW tank (2%–3%) and pumps (1%).

Following the above analysis, on-site constructed SST has a major influence on economic indicators. Therefore, a deeper analysis of the SST is performed where Fig. 14 represents the optimized values for the different SST parameters for each optimal solution. We conclude that $U_{overall} = 0.14\ W/m^2 \cdot K$ is a maximum value for the optimal solution of the largest community size, whereas SST of SDHS for 25 houses community has the lowest $U_{overall} = 0.10\ W/m^2 \cdot K$. Optimal configurations of SST hare listed in Fig. 14, the variation in the parameter values is not consistent with the increase in V_{SST} and community size where the d_{Roof} is around 0.34 m for community size of 10 house and it reduces to 0.12 m, and the d_{Wall} reduces from 0.79 m to 0.6 m. On the other hand, the d_{Gnd} stayed around 0.13 ± 0.02 m. For the SST construction material, the UHPC with $\lambda_{con} = 1.6$ W/m K has a superiority over other construction

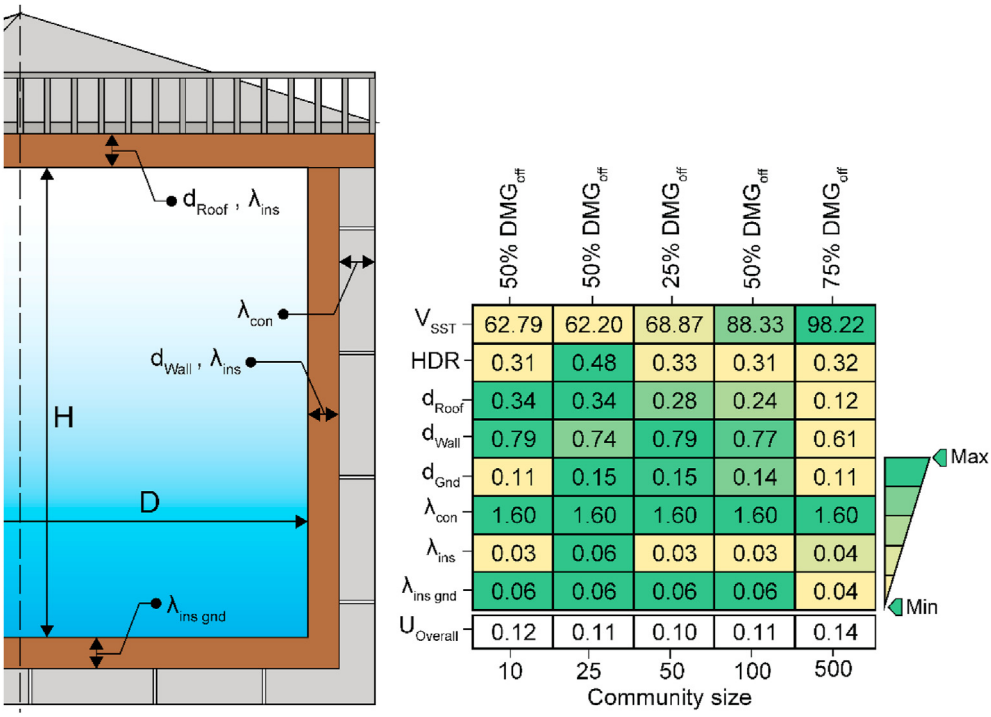

Fig. 14. Design parameters of SST for various community size and optimal solution scenarios.

materials due to its techno-economic and environmental benefits. Regarding the insulation materials, most of the optimal solutions insulate the SST ground using foam glass gravel with thermal conductivity of 0.06 W/m·K. In contrast, the SST walls use the foam glass only at the community size of 25 houses, and other community sizes introduce extruded polystyrene due to its low price. The optimal size of SST for 500 houses community size solution has the most efficient and economical values of design parameters where the SST uses mineral wool in both walls and ground. Thermal performance and the SST's efficiency for the selected optimal solutions are plotted in Fig. 15, where we see an increase in the SST efficiency performance of optimal solutions from 68% at 10 houses up to 89.7% at a community size of 500 houses.

In addition to analyzing the SDHS optimal solutions at different community size, the capability of the methodological optimization framework based on a robust ANN in handling the Heuristics optimization is illustrated through comparing the computational expenses of the optimization process with the SDHS optimization problem mentioned by Tulus et al. [77]. In this study, the average computation time for the anchor points was 15,700 CPU seconds and 47,000 CPU seconds for intermediate Pareto solutions using an Intel® Xeon® E5-2620 v4 2.10 GHz processor with 32.0 GB RAM. In this new framework, the average computational time for developing the full Pareto frontier is only around 600 CPU seconds using the same machine. This huge reduction is due to replacing the TRSNYS model with a robust ANN model and combining it in a MOO framework.

6.4. GSA results

To understand the influence of critical parameters on the objective function, a global sensitivity analysis is performed. The analysis implies BACOO for its low computational cost. Here we have taken 10 houses community size minimum cost-optimal solution as the reference case to study the effects of parameters on the objective function. The reason to select the mentioned case for GSA is to have the closest economic performance to the base case. The parameters for BACOO analysis for GSA (as explained in section 5.2) includes prices of natural gas, electricity, inflation rate for gas and electricity, investment cost, replacement cost, operational cost and discount rate. The effect of these parameters is shown in Fig. 16 on energy performance (Fig. 16a), economic performance (Fig. 16b), environmental performance (Fig. 16c) and on social performance (Fig. 16d). Fig. 16a shows that the energy performance presented by the EPI, which is highly affected by the cost of natural gas and electricity followed by inflation in electricity price, selling cost of electricity to the grid. The main factors affecting the economic performance presented by *IC* are the operational cost, price of natural gas and investment cost. An interesting observation was in the case of environmental performance (represented by *ReCiPe*) where the inflation seemed to affect it greatly, and the other costs (investment, operational and replacement) have a tiny impact on the environment performance under uncertainty (Fig. 16c). Similarly, in Fig. 16d, GSA for social performance indicated that variables like cost of natural gas and electricity have an extreme impact on social performance followed by operational cost, inflation in electricity price and discount rate. Hence, GSA's results cumulatively suggest that natural gas and electricity prices, operational cost, and inflation rates are the most critical factors to ensure the proposed SDHS system's expected performance.

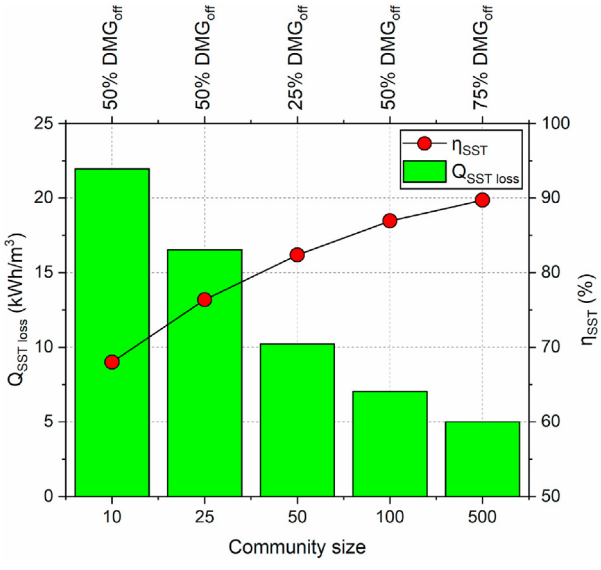

Fig. 15. The annual thermal performance of SST with increased community sizes for optimal solutions.

7. Conclusion

This paper presents an investigation for the sustainable potential of solar assisted district heating system (SDHS) for retrofitted residential communities with different sizes located in Emmen, Netherlands, to achieve Nearly Zero Energy Building (NZEB). The work tends to optimize the performance of SDHS under energy, economic, environmental, and social criteria to facilitate the stakeholders) in the transition from low-carbon buildings (LCBs) to positive energy buildings (PEBs). A machine learning algorithm linked to TRSNYS is developed to simulate the SDHS thermal performance in this context. A multi-objective optimization model is established to minimize the life cycle cost and environmental impact, maximizing green energy use and social benefits. This ensures the system performance and implementation of the smart energy metering system for connecting to the grid. To estimate the SDHS performance from the perspective of sizing, different community sizes (10, 25, 50, 100, 500) were considered under five scenarios representing the effect of cost and environmental damage. A multi-criteria decision-making approach based on TOPSIS (Technique for Order of Preference by Similarity to Ideal Solution) incorporating global sensitivity analysis (GSA) is proposed to help the stakeholders to see beyond the life cycle cost (LCC) and life cycle assessment (LCA) based on selection criteria to choose the most appropriate scenario optimal solution for the desired community size and interpret the effect of various economic parameters on the sustainable performance of SDHS. The summary of the findings is the following:

- Compared to the existing base case (decentralized heat pump), the minimum cost-optimal SDHS solution for 10 houses community size increases by 5.5%, which failed to improve economic potential. However, the environmental performance improved 3.5 times, with 38% more social benefits.
- As the community size increases, more cost-effective and environment-friendly SDHS systems are found. The most environment-friendly optimal SDHS solution for 500 community size is 50% more cost-effective: 450% more environment friendly and has 150% more social benefits compared to the 500 houses community size using the decentralized heat pump.
- The technical analysis of the optimal solution suggests that with the proposed SDHS system, it is possible to achieve a NZEB status for any community size with a solar fraction up to 95% at 500 houses. However, it is possible to achieve PEB status only for

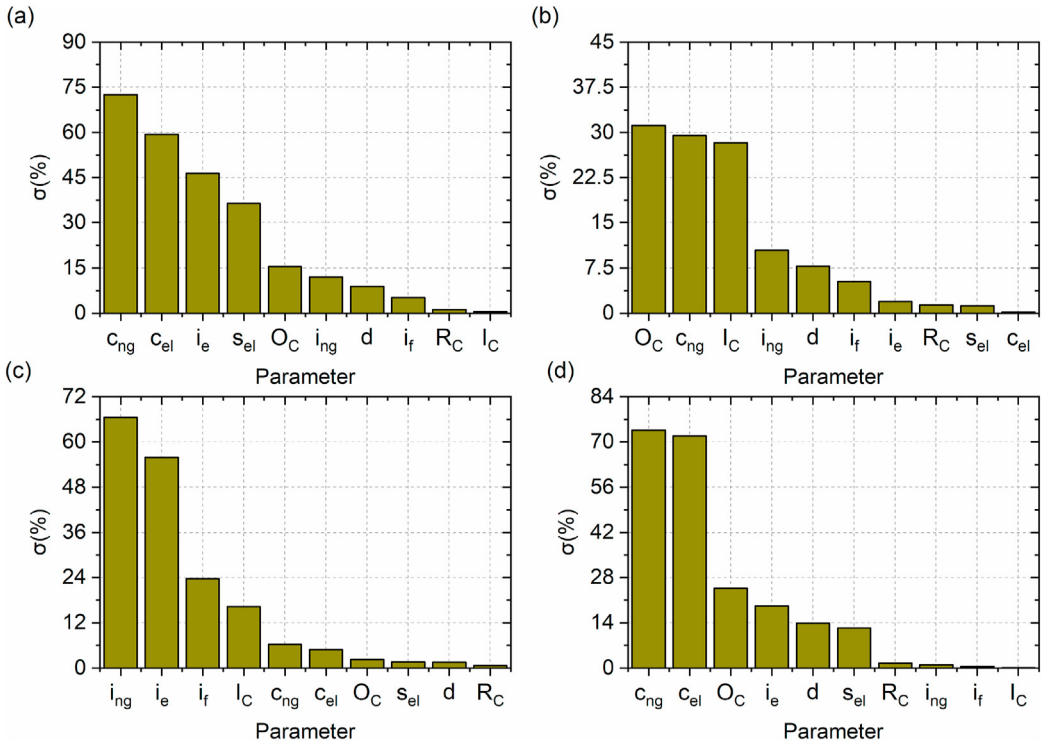

Fig. 16. Results of the global sensitivity analysis following the BACOO method to indicate the influence of critical parameters on (a) Energy indicator; (b) Economic indicator; (c) Environmental indicator; and (d) Social indicator for minimum cost solution of 10 houses community size.

community size higher than 50 houses due to its economic feasibility supported by 25 years of a payback period.

- Economic analysis of the optimal solutions suggests that seasonal storage tank has the biggest impact on the project cost of the SDHS model. In contrast, the environmental analysis shows that PV solar collectors constitute for the greatest part of the environmental impact caused by any optimal SDHS solution.
- Global sensitivity analysis suggests that cumulatively a change in natural gas prices has the highest effect on the SDHS model's economic, environmental, and social performances.
- The adopted methodology has also resulted in providing a guideline for the SDHS system sizing with the optimal size range of SDHS system components.

This work concludes that SDHS provides an attractive renewable energy sources option for cost-effective transitioning to NZEB for medium to long term residential projects. Although the initial investment cost is high, SDHS is comparatively cost-effective in terms of the net present cost. Moreover, our proposed SDHS framework is in line with the 4th generation district heating, which allows for the transition of existing buildings from LCBs to PEBs.

CRediT authorship contribution statement

Mohamed Hany Abokersh: Conceptualization, Methodology, Formal analysis, Software, Data curation, Visualization, Writing – original draft. **Sachin Gangwar:** Formal analysis, Writing – original draft. **Marleen Spiekman:** Data curation, Writing – review & editing. **Manel Vallès:** Conceptualization, Resources, Supervision, Writing – review & editing. **Laureano Jiménez:** Funding acquisition, Writing – review & editing. **Dieter Boer:** Conceptualization, Writing – review & editing, Supervision, Project administration.

Declaration of competing interest

The authors declare that they have no known competing financial interests or personal relationships that could have appeared to influence the work reported in this paper.

Acknowledgements

The work is funded by the Spanish government RTI2018-093849-B-C33 (MCIU/AEI/FEDER, UE). This work is supported by the Ministerio de Ciencia, Innovación y Universidades – Agencia Estatal de Investigación (AEI) (RED2018-102431-T). This project has received funding from the European Union's Horizon 2020 research and innovation programme under the Marie Skłodowska-Curie grant agreement No. 713679 and from the Universitat Rovira i Virgili (URV). In addition, this work was part of the Dutch project TKI Optimaal and co-funded by TKI Urban Energy from the Surcharge for Top Consortia for Knowledge and Innovation (TKIs) of the Ministry of Economic Affairs of the Netherlands.

Appendix A. Supplementary data

Supplementary data to this article can be found online at https://doi.org/10.1016/j.renene.2021.08.091.

References

[1] A. Ghosh, Potential of building integrated and attached/applied photovoltaic (BIPV/BAPV) for adaptive less energy-hungry building's skin: a comprehensive Review, J. Clean. Prod. 276 (2020) 123343, https://doi.org/10.1016/j.jclepro.2020.123343.
[2] M. Abokersh, M. Vallès, L.F. Cabeza, D. Boer, A multicriteria approach to evaluate solar assisted district heating in the German market, in: 14th Int. Conf. Energy Sustain., ASME, 2020, https://doi.org/10.1115/ES2020-1668.
[3] Nearly Zero Energy Building Standard | Business & Public Sector | SEAI, (n.d.).
[4] T. Luo, Y. Tan, C. Langston, X. Xue, Mapping the knowledge roadmap of low

carbon building: a scientometric analysis, Energy Build. 194 (2019) 163–176, https://doi.org/10.1016/j.enbuild.2019.03.050.
[5] R.T. Ely Lecture, B. Nicholas Stern, D. Anderson, A. Bowen, S. Catovsky, P. Diamond, S. Dietz, O. Edenhofer, S. Fankhauser, G. Floater, S.-L. Garbett, R. Garnaut, R. Guesnerie, G. Heal, D. Hawellek, C. Henry, C. Hepburn, P. Joskow, J.-P. Landau, J. Mirrlees, E. Moniz, S. Pacala, N. Patmore, V. Pope, L. Ralston, M. Romani, J. Schellnhuber, M. Skellern, R. Socolow, M. Weitzman, The Economics of Climate Change, 2008.
[6] E. Commission, 2 Energy Efficiency State of Non-profit Housing Stock in the Netherlands, 2020, pp. 61–82.
[7] X. Lai, J. Liu, Q. Shi, G. Georgiev, G. Wu, Driving forces for low carbon technology innovation in the building industry: a critical review, Renew. Sustain. Energy Rev. 74 (2017) 299–315, https://doi.org/10.1016/j.rser.2017.02.044.
[8] J. Al Dakheel, C. Del Pero, N. Aste, F. Leonforte, Smart buildings features and key performance indicators: a review, Sustain. Cities Soc. 61 (2020) 102328, https://doi.org/10.1016/j.scs.2020.102328.
[9] A. Hamburg, K. Kuusk, A. Mikola, T. Kalamees, Realisation of energy performance targets of an old apartment building renovated to nZEB, Energy 194 (2020) 116874, https://doi.org/10.1016/j.energy.2019.116874.
[10] H. Lund, P.A. Østergaard, M. Chang, S. Werner, S. Svendsen, P. Sorknæs, J.E. Thorsen, F. Hvelplund, B.O.G. Mortensen, B.V. Mathiesen, C. Bojesen, N. Duic, X. Zhang, B. Möller, The status of 4th generation district heating: research and results, Energy 164 (2018) 147–159, https://doi.org/10.1016/j.energy.2018.08.206.
[11] H. Lund, N. Duic, P.A. Østergaard, B.V. Mathiesen, Future District Heating Systems and Technologies: on the Role of Smart Energy Systems and 4th Generation District Heating, Energy (2018), https://doi.org/10.1016/j.energy.2018.09.115.
[12] H. Lund, S. Werner, R. Wiltshire, S. Svendsen, J.E. Thorsen, F. Hvelplund, B.V. Mathiesen, 4th Generation District Heating (4GDH). Integrating smart thermal grids into future sustainable energy systems, Energy 68 (2014) 1–11, https://doi.org/10.1016/j.energy.2014.02.089.
[13] H. Li, N. Nord, Transition to the 4th generation district heating - possibilities, bottlenecks, and challenges, in: Energy Procedia, 2018, https://doi.org/10.1016/j.egypro.2018.08.213.
[14] M. Ferrara, F. Della Santa, M. Bilardo, A. De Gregorio, A. Mastropietro, U. Fugacci, F. Vaccarino, E. Fabrizio, Design optimization of renewable energy systems for NZEBs based on deep residual learning, Renew. Energy 176 (2021) 590–605, https://doi.org/10.1016/j.renene.2021.05.044.
[15] I.A. Gondal, Prospects of Shallow geothermal systems in HVAC for NZEB, Energy Built Environ (2020), https://doi.org/10.1016/j.enbenv.2020.09.007.
[16] B. Grillone, S. Danov, A. Sumper, J. Cipriano, G. Mor, A review of deterministic and data-driven methods to quantify energy efficiency savings and to predict retrofitting scenarios in buildings, Renew. Sustain. Energy Rev. 131 (2020) 110027, https://doi.org/10.1016/j.rser.2020.110027.
[17] A. Magrini, G. Lentini, S. Cuman, A. Bodrato, L. Marenco, From nearly zero energy buildings (NZEB) to positive energy buildings (PEB): the next challenge - the most recent European trends with some notes on the energy analysis of a forerunner PEB example, Dev. Built Environ. 3 (2020) 100019, https://doi.org/10.1016/j.dibe.2020.100019.
[18] A. Behzadi, A. Arabkoohsar, Y. Yang, Optimization and dynamic techno-economic analysis of a novel PVT-based smart building energy system, Appl. Therm. Eng. 181 (2020) 115926, https://doi.org/10.1016/j.applthermaleng.2020.115926.
[19] A. Behzadi, A. Arabkoohsar, Feasibility study of a smart building energy system comprising solar PV/T panels and a heat storage unit, Energy 210 (2020) 118528, https://doi.org/10.1016/j.energy.2020.118528.
[20] M.H. Abokersh, K. Saikia, L.F. Cabeza, D. Boer, M. Vallès, Flexible heat pump integration to improve sustainable transition toward 4th generation district heating, Energy Convers. Manag. 225 (2020), https://doi.org/10.1016/j.enconman.2020.113379.
[21] M. Hany, M. Spiekman, O. Vijlbrief, T.A.J. Van Goch, M. Vall, D. Boer, A Real-Time Diagnostic Tool for Evaluating the Thermal Performance of Nearly Zero Energy Buildings, 2021, p. 281, https://doi.org/10.1016/j.apenergy.2020.116091.
[22] D. Majcen, L.C.M. Itard, H. Visscher, Theoretical vs. actual energy consumption of labelled dwellings in The Netherlands: discrepancies and policy implications, Energy Pol. 54 (2013) 125–136, https://doi.org/10.1016/j.enpol.2012.11.008.
[23] T. Hong, M. Lee, C. Koo, K. Jeong, J. Kim, Development of a method for estimating the rooftop solar photovoltaic (PV) potential by analyzing the available rooftop area using Hillshade analysis, Appl. Energy 194 (2017) 320–332, https://doi.org/10.1016/j.apenergy.2016.07.001.
[24] J. Jeong, T. Hong, J. Kim, M. Chae, C. Ji, Multi-criteria analysis of a self-consumption strategy for building sectors focused on ground source heat pump systems, J. Clean. Prod. 186 (2018) 68–80, https://doi.org/10.1016/j.jclepro.2018.03.121.
[25] H. ur Rehman, J. Hirvonen, K. Sirén, Performance comparison between optimized design of a centralized and semi-decentralized community size solar district heating system, Appl. Energy 229 (2018) 1072–1094, https://doi.org/10.1016/j.apenergy.2018.08.064.
[26] X. Cao, X. Dai, J. Liu, Building energy-consumption status worldwide and the state-of-the-art technologies for zero-energy buildings during the past decade, Energy Build. 128 (2016) 198–213, https://doi.org/10.1016/j.enbuild.2016.06.089.
[27] A.J. Marszal, P. Heiselberg, R. Lund Jensen, J. Nørgaard, On-site or off-site renewable energy supply options? Life cycle cost analysis of a Net Zero Energy Building in Denmark, Renew. Energy 44 (2012) 154–165, https://doi.org/10.1016/j.renene.2012.01.079.
[28] S. Susan, D. Wardhani, Building integrated photovoltaic as GREENSHIP'S on site renewable energy tool, Results Eng 7 (2020) 100153, https://doi.org/10.1016/j.rineng.2020.100153.
[29] J. Song, S.D. Oh, S.J. Song, Effect of increased building-integrated renewable energy on building energy portfolio and energy flows in an urban district of Korea, Energy 189 (2019) 116132, https://doi.org/10.1016/j.energy.2019.116132.
[30] G. Barone, A. Buonomano, C. Forzano, G.F. Giuzio, A. Palombo, Passive and active performance assessment of building integrated hybrid solar photovoltaic/thermal collector prototypes: energy, comfort, and economic analyses, Energy 209 (2020) 118435, https://doi.org/10.1016/j.energy.2020.118435.
[31] G. Li, Q. Xuan, M.W. Akram, Y. Golizadeh Akhlaghi, H. Liu, S. Shittu, Building integrated solar concentrating systems: a review, Appl. Energy 260 (2020) 114288, https://doi.org/10.1016/j.apenergy.2019.114288.
[32] T.E. Kuhn, C. Erban, M. Heinrich, J. Eisenlohr, F. Ensslen, D.H. Neuhaus, Review of technological design options for building integrated photovoltaics (BIPV), Energy Build (2020) 110381, https://doi.org/10.1016/j.enbuild.2020.110381.
[33] S. Dawood, T. Crosbie, N. Dawood, R. Lord, Designing low carbon buildings: a framework to reduce energy consumption and embed the use of renewables, Sustain. Cities Soc. 8 (2013) 63–71, https://doi.org/10.1016/j.scs.2013.01.005.
[34] Y. Sun, P. Huang, G. Huang, A multi-criteria system design optimization for net zero energy buildings under uncertainties, Energy Build. 97 (2015) 196–204, https://doi.org/10.1016/j.enbuild.2015.04.008.
[35] C. Mokhtara, B. Negrou, N. Settou, A. Gouareh, B. Settou, Pathways to plus-energy buildings in Algeria: design optimization method based on GIS and multi-criteria decision-making, in: Energy Procedia, Elsevier Ltd, 2019, pp. 171–180, https://doi.org/10.1016/j.egypro.2019.04.019.
[36] L. Laguna Salvad, E. Villeneuve, D. Masson, Decision making in near zero energy building refurbishment: a technology alternatives ranking tool, IFAC-PapersOnLine. 52 (2019) 313–318, https://doi.org/10.1016/j.ifacol.2019.11.196.
[37] Y. Chang, Y. Wei, The utilization of renewable energy for low-carbon buildings, in: Renewable-Energy-Driven Futur, Elsevier, 2021, pp. 289–309, https://doi.org/10.1016/B978-0-12-820539-6.00009-1.
[38] M. Pinamonti, P. Baggio, Energy and economic optimization of solar-assisted heat pump systems with storage technologies for heating and cooling in residential buildings, Renew. Energy 157 (2020) 90–99, https://doi.org/10.1016/j.renene.2020.04.121.
[39] H. Li, S. Wang, Coordinated optimal design of zero/low energy buildings and their energy systems based on multi-stage design optimization, Energy 189 (2019) 116202, https://doi.org/10.1016/j.energy.2019.116202.
[40] Y. Zhou, S. Zheng, Z. Liu, T. Wen, Z. Ding, J. Yan, G. Zhang, Passive and active phase change materials integrated building energy systems with advanced machine-learning based climate-adaptive designs, intelligent operations, uncertainty-based analysis and optimisations: a state-of-the-art review, Renew. Sustain. Energy Rev. 130 (2020) 109889, https://doi.org/10.1016/j.rser.2020.109889.
[41] Y. Bengio, A. Lodi, A. Prouvost, Machine learning for combinatorial optimization: a methodological tour d'horizon, Eur. J. Oper. Res. (2020), https://doi.org/10.1016/j.ejor.2020.07.063.
[42] H. ur Rehman, T. Korvola, R. Abdurafikov, T. Laakko, A. Hasan, F. Reda, Data analysis of a monitored building using machine learning and optimization of integrated photovoltaic panel, battery and electric vehicles in a Central European climatic condition, Energy Convers. Manag. 221 (2020) 113206, https://doi.org/10.1016/j.enconman.2020.113206.
[43] H. Han, Z. Zhang, X. Cui, Q. Meng, Ensemble learning with member optimization for fault diagnosis of a building energy system, Energy Build. 226 (2020) 110351, https://doi.org/10.1016/j.enbuild.2020.110351.
[44] S. Seyedzadeh, F. Pour Rahimian, S. Oliver, S. Rodriguez, I. Glesk, Machine learning modelling for predicting non-domestic buildings energy performance: a model to support deep energy retrofit decision-making, Appl. Energy 279 (2020) 115908, https://doi.org/10.1016/j.apenergy.2020.115908.
[45] S. Fathi, R. Srinivasan, A. Fenner, S. Fathi, Machine learning applications in urban building energy performance forecasting: a systematic review, Renew. Sustain. Energy Rev. 133 (2020) 110287, https://doi.org/10.1016/j.rser.2020.110287.
[46] M. Mishra, Machine learning techniques for structural health monitoring of heritage buildings: a state-of-the-art review and case studies, J. Cult. Herit. (2020), https://doi.org/10.1016/j.culher.2020.09.005.
[47] H. Sun, H.V. Burton, H. Huang, Machine learning applications for building structural design and performance assessment: state-of-the-art review, J. Build. Eng. 33 (2020) 101816, https://doi.org/10.1016/j.jobe.2020.101816.
[48] M. Ayoub, A review on machine learning algorithms to predict daylighting inside buildings, Sol. Energy 202 (2020) 249–275, https://doi.org/10.1016/j.solener.2020.03.104.
[49] T. Hong, Z. Wang, X. Luo, W. Zhang, State-of-the-art on research and applications of machine learning in the building life cycle, Energy Build. 212 (2020) 109831, https://doi.org/10.1016/j.enbuild.2020.109831.
[50] G. Mavromatidis, K. Orehounig, J. Carmeliet, Uncertainty and global sensitivity analysis for the optimal design of distributed energy systems, Appl. Energy 214 (2018) 219–238, https://doi.org/10.1016/j.apenergy.2018.01.062.

[51] C. You, J. Kim, Optimal design and global sensitivity analysis of a 100% renewable energy sources based smart energy network for electrified and hydrogen cities, Energy Convers. Manag. 223 (2020) 113252, https://doi.org/10.1016/j.enconman.2020.113252.
[52] Y. Zhang, X. Zhang, P. Huang, Y. Sun, Global sensitivity analysis for key parameters identification of net-zero energy buildings for grid interaction optimization, Appl. Energy 279 (2020) 115820, https://doi.org/10.1016/j.apenergy.2020.115820.
[53] S.A. Klein, et al., TRNSYS Version. 18, Solar Energy Laboratory, University of Wisconsin-Madison, 2004. Website, http://sel.me.wisc.edu/trnsys.
[54] D.B. Mh Abokersh, M. Vallès, L.F. Cabeza, Challenges associated with the construction and operation of seasonal storage for A small solar district heating system: a multi-objective optimization approach, in: 14th Int. Renew. Energy Storage Conf. 2020 (IRES 2020), IRES 2020, 2020, pp. 150–160, https://doi.org/10.2991/ahe.k.210202.023.
[55] V. Tulus, D. Boer, L.F. Cabeza, L. Jiménez, G. Guillén-Gosálbez, Enhanced thermal energy supply via central solar heating plants with seasonal storage: a multi-objective optimization approach, Appl. Energy 181 (2016) 549–561, https://doi.org/10.1016/j.apenergy.2016.08.037.
[56] M.H. Abokersh, M. Spiekman, O. Vijlbrief, T.A.J. van Goch, M. Vallès, D. Boer, A real-time diagnostic tool for evaluating the thermal performance of nearly zero energy buildings, Appl. Energy 281 (2021), https://doi.org/10.1016/j.apenergy.2020.116091.
[57] J. Hadorn, Guide to Seasonal Heat Storage, SIA, Swiss Association of Engineers and Architects, Zurich, 1990.
[58] M.H. Abokersh, M. Vallès, L.F. Cabeza, D. Boer, A framework for the optimal integration of solar assisted district heating in different urban sized communities : a robust machine learning approach incorporating global sensitivity analysis, Appl. Energy 267 (2020) 114903, https://doi.org/10.1016/j.apenergy.2020.114903.
[59] G. De Luca, I. Ballarini, A. Lorenzati, V. Corrado, Renovation of a social house into a NZEB: use of renewable energy sources and economic implications, Renew. Energy 159 (2020) 356–370, https://doi.org/10.1016/j.renene.2020.05.170.
[60] G. Guillen-Gosalbez, J.A. Caballero, L.J. Esteller, M. Gadalla, Application of life cycle assessment to the structural optimization of process flowsheets, Comput. Aided Chem. Eng. 24 (2007) 1163–1168, https://doi.org/10.1016/S1570-7946(07)80218-5.
[61] M.A.J. Huijbregts, Z.J.N. Steinmann, P.M.F. Elshout, G. Stam, F. Verones, M. Vieira, M. Zijp, A. Hollander, R. van Zelm, ReCiPe2016: a harmonised life cycle impact assessment method at midpoint and endpoint level, Int. J. Life Cycle Assess. 22 (2017) 138–147, https://doi.org/10.1007/s11367-016-1246-y.
[62] A.P. Gursel, C. Ostertag, Comparative life-cycle impact assessment of concrete manufacturing in Singapore, Int. J. Life Cycle Assess. (2017), https://doi.org/10.1007/s11367-016-1149-y.
[63] Y. Chen, J. Wang, P.D. Lund, Sustainability evaluation and sensitivity analysis of district heating systems coupled to geothermal and solar resources, Energy Convers. Manag. 220 (2020) 113084, https://doi.org/10.1016/j.enconman.2020.113084.
[64] L. Cameron, B. Van Der Zwaan, Employment factors for wind and solar energy technologies: a literature review, Renew. Sustain. Energy Rev. 45 (2015) 160–172, https://doi.org/10.1016/j.rser.2015.01.001.
[65] D. Bauer, R. Marx, J. Nußbicker-Lux, F. Ochs, W. Heidemann, H. Müller-Steinhagen, German central solar heating plants with seasonal heat storage, Sol. Energy 84 (2010) 612–623, https://doi.org/10.1016/j.solener.2009.05.013.
[66] A multiobjective simplex method, in: Multicriteria Optim., Springer-Verlag, 2005, pp. 171–196, https://doi.org/10.1007/3-540-27659-9_7.
[67] K. Nö, S. Niedenfü Hr, M. Beyß Id, W. Wiechert Id, A Pareto Approach to Resolve the Conflict between Information Gain and Experimental Costs: Multiple-Criteria Design of Carbon Labeling Experiments, 2018, https://doi.org/10.1371/journal.pcbi.1006533.
[68] A. Alajmi, J. Wright, Selecting the most efficient genetic algorithm sets in solving unconstrained building optimization problem, Int. J. Sustain. Built Environ. 3 (2014) 18–26, https://doi.org/10.1016/j.ijsbe.2014.07.003.
[69] A. Saltelli, P. Annoni, How to avoid a perfunctory sensitivity analysis, Environ. Model. Software 25 (2010) 1508–1517, https://doi.org/10.1016/j.envsoft.2010.04.012.
[70] N. Lior, Sustainability as the Quantitative Norm for Water Desalination Impacts, 2017, https://doi.org/10.1016/j.desal.2016.08.008.
[71] V. Campos-Guzmán, M.S. García-Cáscales, N. Espinosa, A. Urbina, Life Cycle Analysis with Multi-Criteria Decision Making: a review of approaches for the sustainability evaluation of renewable energy technologies, Renew. Sustain. Energy Rev. 104 (2019) 343–366, https://doi.org/10.1016/j.rser.2019.01.031.
[72] C. Bhowmik, S. Gangwar, S. Bhowmik, A. Ray, Selection of Energy-Efficient Material: an Entropy–TOPSIS Approach, 2018, https://doi.org/10.1007/978-981-10-5699-4_4.
[73] C.-L. Hwang, K. Yoon, Methods for Multiple Attribute Decision Making, 1981, pp. 58–191, https://doi.org/10.1007/978-3-642-48318-9_3.
[74] F. Sari, Forest fire susceptibility mapping via multi-criteria decision analysis techniques for Mugla, Turkey: a comparative analysis of VIKOR and TOPSIS, For. Ecol. Manage. 480 (2021) 118644, https://doi.org/10.1016/j.foreco.2020.118644.
[75] X. Qin, H. Wang, Y. Li, Y. Li, B. McConkey, R. Lemke, C. Li, K. Brandt, Q. Gao, Y. Wan, S. Liu, Y. Liu, C. Xu, A long-term sensitivity analysis of the denitrification and decomposition model, Environ. Model. Software 43 (2013) 26–36, https://doi.org/10.1016/j.envsoft.2013.01.005.
[76] M.H. Abokersh, M. Vallès, L. Jiménez, D. Boer, Cost-Effective Processes of Solar District Heating System Based on Optimal Artificial Neural Network, 2020, https://doi.org/10.1016/B978-0-12-823377-1.50068-9.
[77] V. Tulus, M.H. Abokersh, L.F. Cabeza, M. Vallès, L. Jiménez, D. Boer, Economic and environmental potential for solar assisted central heating plants in the EU residential sector: contribution to the 2030 climate and energy EU agenda, Appl. Energy (2019), https://doi.org/10.1016/j.apenergy.2018.11.094.